Doctoral Dissertation

(Shinshu University)

Studies on roles of lysophosphatidylethanolamine in neuronal morphology and survival

September 2021

Kazutoshi Hisano

Department of Biomedical Engineering,
Graduate School of Medicine, Science and Technology

Table of Contents

Chapter 1 Background

1-1 Neural circuits 4

1-1-1 Central nervous system neuron 4

1-1-2 Neurite outgrowth 5

1-2 The importance of phospholipids in the brain 7

1-2-1 Brain phospholipids 7

1-2-2 Role of phospholipids in neurons 8

1-2-3 Phospholipids and diseases 10

1-3 The composition of this thesis 11

Chapter 2

Structurally different lysophosphatidylethanolamine species stimulate neurite outgrowth in cultured cortical neurons via distinct G-protein-coupled receptors and signaling cascades

2-1 Abstract 14

2-2 Introduction 15

2-3 Result 17

2-3-1 Effects of phospholipids on neuronal morphology 17

2-3-2 Effects of 16:0 LPE and 18:0 LPE on neuronal morphology 20

2-3-3 Effects of 16:0 LPE and 18:0 LPE on neurite outgrowth 22

2-3-4 LPEs activate MAPK in cultured cortical neurons. 25

2-3-5 Effects of MAPK inhibitor on LPE-stimulated neurite outgrowth 27

2-3-6 Effects of G-protein and enzyme inhibitors on LPE-stimulated neurite outgrowth 29

2-4 Discussion 32

2-5 Material and Methods 35

Chapter 3

Abundant oleoyl-lysophosphatidylethanolamine in brain stimulates neurite outgrowth and protects against glutamate toxicity in cultured cortical neurons

3-1 Abstract.....40
3-2 Introduction.....41
3-3 Result.....43
3-3-1 Comprehensive LC-ESI-MS/MS analysis of LPE species in 4-week-old mice brain.....43
3-3-2 Effects of 18:1 LPE on neurite outgrowth.....44
3-3-3 Effects of inhibitors on 18:1 LPE-stimulated neurite outgrowth.....47
3-3-4 18:1 LPE activate MAPK in cultured cortical neurons.....50
3-3-5 Protective effect of 18:1 LPE on glutamate-induced neurotoxicity.....52
3-4 Discussion.....57
3-5 Material and Methods.....62

4 Conclusion..... 67

5 Bibliography..... 68

6 Acknowledgments..... 76

List of abbreviations

AKT: Serine/threonine kinase Akt

AraC: 4 μM 1-β-D-arabino-furanosyl-cytosine

CB: cerebrosides

CNS: central nervous system

CL: cardiolipin

DIV: days in vitro

ERK: extracellular signal-regulated kinase

GPCRs: G-protein coupled receptors

LC-ESI-MS/MS: liquid chromatography-electrospray ionization tandem mass spectrometry analysis

LPA: Lysophosphatidic acid

LPC: lysophosphatidylcholine

LPE: lysophosphatidylethanolamine

MAP2: microtubule-associated protein 2

MAPK: p42/p44 mitogen-activated protein kinase

NeuN: neuronal nuclear antigen

PA: phosphatidic acid

PBS: phosphate-buffered saline

PC: phosphatidylcholine

PE: phosphatidylethanolamine

PI3K: Phosphatidylinositol-3 kinase

PI: phosphatidylinositol

PKC: protein kinase C

PLC: phospholipase C

PS: phosphatidylserine

PTX: pertussis toxin

S1P: sphingosine-1-phosphate

Chapter 1 Background

1-1 Neural circuits

1-1-1 Central nervous system neuron

The human brain consists of a complex network of neurons. These neurons serve as the building blocks of the nervous system, transmitting information to and from the brain and throughout the body. Neurons are divided into (1) soma, (2) dendrite, (3) axon, and (4) synapse (**Fig. 1**).

(1) Soma: The soma is the body of the neuron. It contains intracellular structures called organelles that include the nucleus. Most protein synthesis occurs here. The role of the soma is to provide energy for the cell to keep it alive and make repairs.

(2) Dendrite: The dendrite begins at the soma and extend outwards, like the branches of a tree. Dendrites receive impulses from the axon terminal of the adjoining neurons. They carry impulses to the nucleus or soma.

(3) Axon: The axon is a long and slender branch compared with the dendrites. The transmitting part of the neuron. Axons carry electrical impulses from the soma to the synapse.

(4) Synapse: The synapses are intercellular junctions between a presynaptic neuron and a postsynaptic cell, usually also a neuron. In many synapses, the presynaptic part is located on an axon and the postsynaptic part is located on a dendrite. It is a structure that allows the neuron to pass an electrical/chemical signal to another neuron.

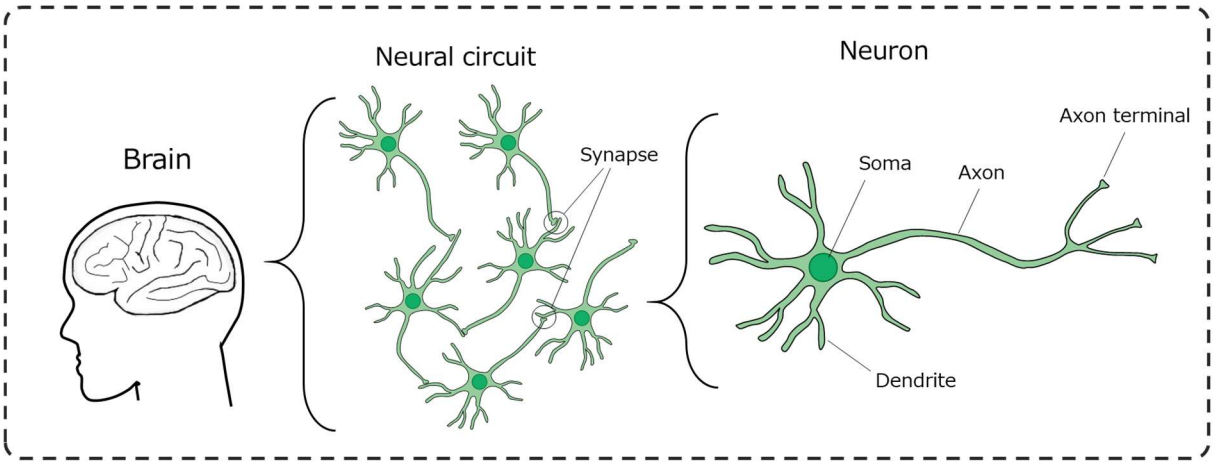

Fig.1 Neural Circuits.

During brain development, neurons become assembled into functional networks by growing axons and dendrites (collectively called neurites) that connect synapses to other neurons. For the nervous system to function correctly, it is extremely important that the neurons have the correct morphology and establish the appropriate connections. The interaction between different neurons in the brain is needed to communicate and process information according to what we see, hear, think, and move.

1-1-2 Neurite outgrowth

Neurite outgrowth is an important process for neuronal wiring during development and synaptic plasticity under physiological conditions, and for regeneration of neuronal wiring following trauma and disease in the brain [**1–4**].

As far, many signaling molecules have been identified to be involved in neurite outgrowth. It has been reported that many ligands including neurotrophins, Wnt proteins, neurotransmitters, hormones, and neuropeptides have been identified that stimulate neurite outgrowth via binding to their receptors [**5–11**]. Binding of these ligands to the receptors stimulates various intracellular protein kinases that control

neurite outgrowth such as MAPK (Mitogen-activated protein kinase), AKT (Serine/threonine kinase Akt), PI3K (Phosphatidylinositol-3 kinase), PKC (Protein kinase C) and PKA (Protein kinase A) [**12**]. In addition, these processes allow activation or deactivation of signaling pathway and play integral roles in the neurite outgrowth regulatory pathway. Although, numerous studies had been focused on identification of the molecules that regulate neurite outgrowth and clarifying their mechanism, however it remains unclear.

Outgrowth of neurites (including both axons and dendrites) is a fundamental event in the formation of neural circuits. Neural circuits are the basis of neural function in health and disease, and the incomplete assembly or disintegration of these circuits can cause disorders of the nervous system.

For example, neurodevelopmental disorders such as intellectual disability, autism spectrum disorders, and schizophrenia are associated with abnormal development of neural circuits. In addition, neurodegenerative diseases such as Alzheimer's disease and Parkinson's disease are caused by disintegration of neural circuits [**13–16**].

Thus, identifying the molecules that regulate neurite outgrowth and clarifying their mechanism are essential for understanding of mechanism of neuronal wiring and brain functions, and for development of therapeutics of neurological disorders.

1-2 The importance of phospholipids in the brain

1-2-1 Brain phospholipids

Lipids have a variety of biological roles. They serve as fuel molecules, highly concentrated energy stores, signal molecules, and components of membranes. In the brain, lipids are major components of comprising 40-55% of the dry matter present, with phospholipids making up half of total brain lipid. The phospholipid composition of the top three phospholipids found in the adult brain is approximately 35-40% Phosphatidylcholine (PC), 35-40% Phosphatidylethanolamine (PE) and 20% Phosphatidylserine (PS) [**17**].

Phospholipids are structurally and functionally important constituents of brains. In general, phospholipids are composed of a glycerol backbone, two hydrophobic fatty acid tails, a hydrophilic head containing a phosphate group. The type of the head group identifies the phospholipid, with choline, ethanolamine, serine, inositol, or glycerol groups capable of addition (**Fig. 2**). The hydrolysis of one of the two fatty acids gives rise to the lipid species as lysophospholipids. Various enzymes are involved in the synthesis and metabolism of phospholipids (**Fig. 3**) [**18**, **19**].

In human brain, many types of phospholipid species are present due to the combination of phospholipid headgroups and fatty acids. Such structural diversity affects the properties including membrane fluidity and the regulation of membrane-bound protein activity [**18–20**].

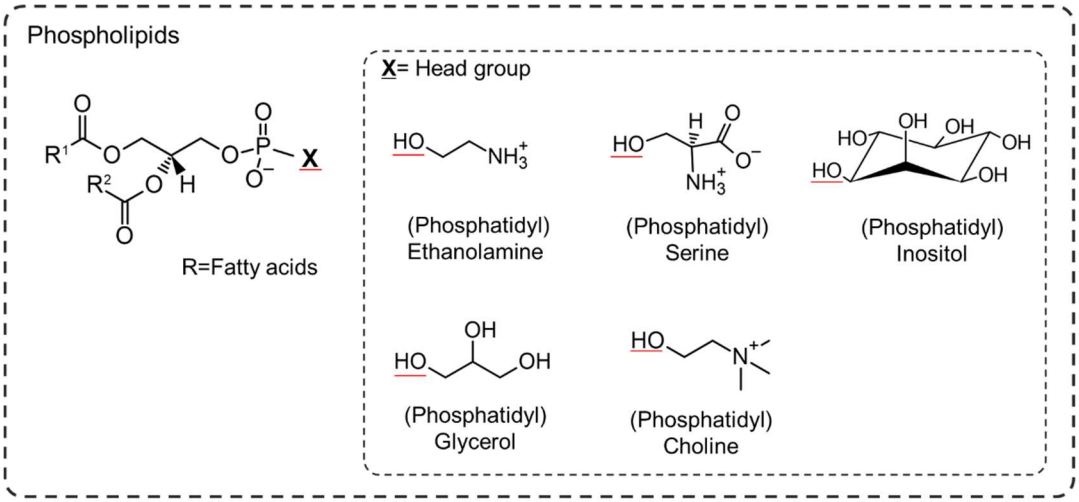

Fig.2 Schematic overview of phospholipid structure.

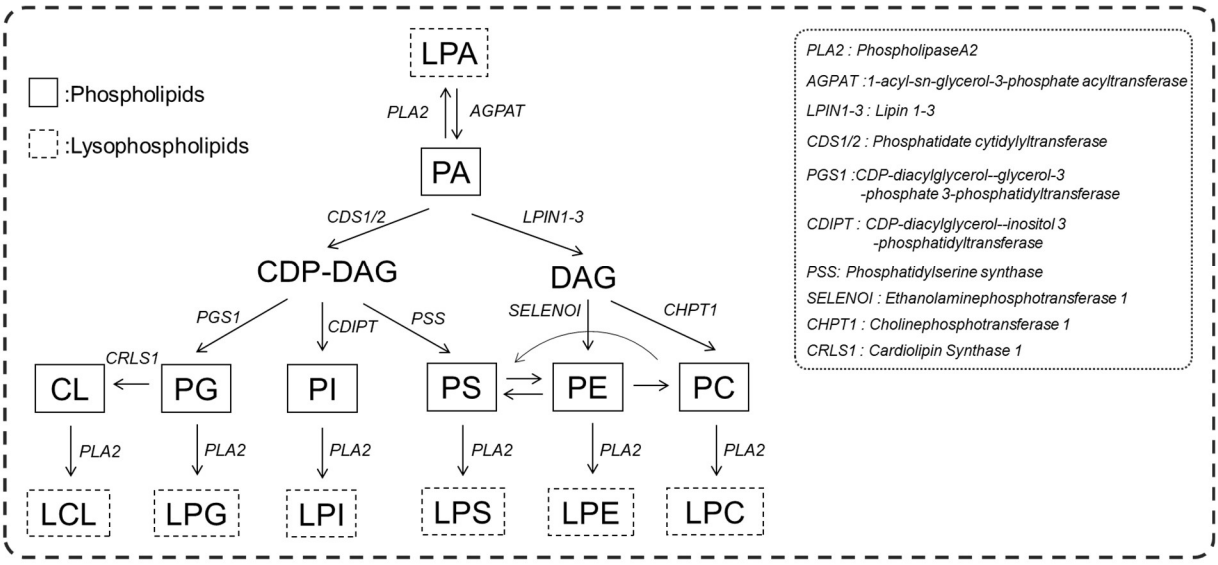

Fig.3 Schematic overview of phospholipid synthesis.

PA (phosphatidic acid), LPA (lysophosphatidic acid), CDP-DAG (cytidine diphosphate diacylglycerol), DAG (diacylglycerol), CL (cardiolipin), LPL (lysocardiolipin), PG (phosphoglycerol) , LPG (lysophosphoglycerol), PI (phosphatidylinositol), LPI (lysophosphatidylinositol), PS (phosphatidylserine), LPS (lysophosphatidylserine), PE (phosphatidylethanolamine), LPE (lysophosphatidylethanolamine), PC (phosphatidylcholine), LPC (lysophosphatidylcholine).

1-2-2 Role of phospholipids in neurons

Phospholipids are thought to play an important role in neurons. Some examples as follows. PC is served as a reservoir of neurotransmitter, acetylcholine. Acetylcholine functions as a neurotransmitter and neuromodulator. The brain has several cholinergic areas, and it plays an important role in arousal, attention, memory, and motivation [**18**]. PS participates in key signaling pathways in the neuronal system. PS is involved in the activation of Akt, Raf/Ras and PKC signaling, which supports neuronal survival and differentiation [**21**].

Recently, among the physiologically active phospholipids, the role of lysophospholipids in biological functions has attracted attention. Lysophospholipids are consisting of a hydrophilic head group and one hydrophobic fatty acid chain and are produced by phospholipase A-type reaction. Many lysophospholipid molecular species exist in the brain (**Fig. 4**) [**22–23**].

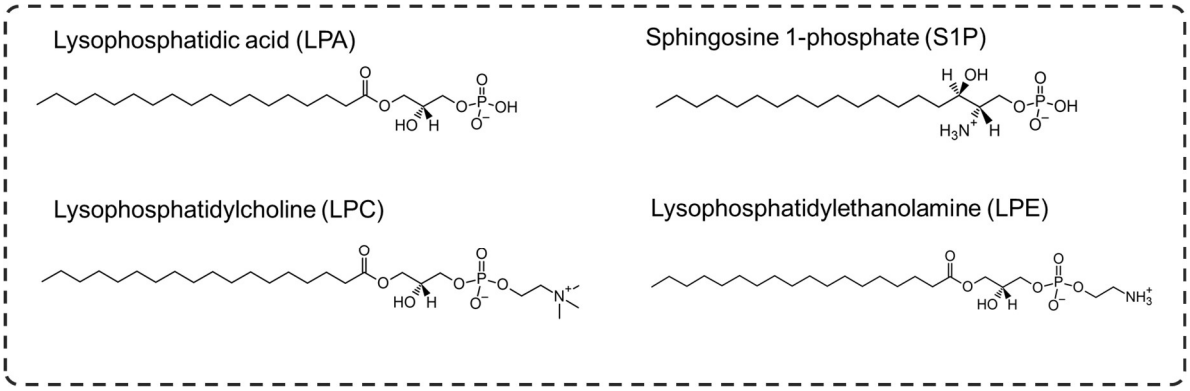

Fig.4 Schematic representation of structure of lysophospholipids. Each containing stearic acid (18:0) is shown.

Two of the best studied lysophospholipids are lysophosphatidic acid (LPA) and sphingosine-1-phosphate (S1P). These lysophospholipids have been reported to act extracellularly as an agonist on their membrane receptor. These two lysophospholipids are previously known as biosynthetic metabolites of cell membrane phospholipids, but they are now regarded as important regulators for diverse biological functions through activation of their specific receptors. It has been reported that these functions are mediated via specific G-protein coupled receptors (GPCRs), which are widely distributed throughout the body including CNS neurons [**23**].

In vitro neuron culture studies have reported that the effects of LPA and S1P signaling are largely related to morphological changes involving growth cone collapse, neurite retraction, synapse formation and synapse transmission [**23–26**]. However, other lysophospholipids such as Lysophosphatidylcholine (LPC) and lysophosphatidylethanolamine (LPE), the roles of these lysophospholipids in neuron remain largely unknown.

1-2-3 Phospholipids and diseases

Recently, it has been suggested that metabolic changes of phospholipids are highly associated with brain diseases. Some reports show that cognitive impairment or traumatic brain damage is associated with an imbalance in the composition of phospholipids in the brain, in which some studies have reported changes of phospholipid levels in the brain. Postischemic cognitive impairment rat model shows increasement of LPE and PS, and decreasement of PC in the hippocampus [**27**]. Lipid profiling investigation in major depressive disorder subjects reported that lysophospholipids (LPC and LPE) and phospholipids (PC, PE and PI) are changed in the serums [**28**]. Traumatic brain injury rats show changes in the levels of the PE, PS and LPE in the injury area [**29**]. In addition, in Parkinson's disease and Alzheimer's disease, changes in lipid levels, including phospholipids, have been observed in these patients [**19**, **30**].

These observations imply the importance of phospholipids in the brain in normal development, as well as in pathological settings. Comprehensive analysis of phospholipids in the brain and investigation of their functions are necessary to understand their roles in physiological and pathophysiological conditions.

1-3 The composition of this thesis

The overall aim of this thesis is to identify and characterize phospholipids that regulate neuronal morphology and survival in CNS neurons.

To achieve the aims of this thesis, using commercially available phospholipid kit containing 10 different phospholipids, I examined the effects of phospholipids on neuronal morphology. I found that LPE strongly stimulates both axonal and dendritic outgrowth in cultured cortical neurons (**Chapter 2-3-1**). Next, I examined whether palmitoyl-LPE (16:0 LPE) or stearoyl-LPE (18:0 LPE) effects on neuronal morphology. I found that structurally distinct LPE species 16:0 LPE and 18:0 LPE both increase axonal and dendritic outgrowth in cultured cortical neurons (**Chapter 2-3-2**). Then, the effects of 16:0 LPE and 18:0 LPE on neurite outgrowth were examined by directly measuring the length of neurites. I found that LPEs have strong activity for promoting neurite outgrowth in the cultured cortical neurons (**Chapter 2-3-3**). To examine whether 16:0 LPE and 18:0 LPE activate MAPK/ERK1/2, I subjected to western blot analysis. Both 16:0 LPE and 18:0 LPE activate MAPK/ERK1/2 to the same extent, but the effect of the MAPK inhibitor differed between the 16:0 LPE- and 18:0 LPE-treated culture. MAPK inhibitor completely inhibited 18:0 LPE-induced neurite outgrowth and partially inhibited 16:0 LPE-induced neurite outgrowth (**Chapter 2-3-4 and 2-3-5**). Then, using G proteins inhibitor, I examined whether the G protein-coupled receptors are involved in the actions of 16:0 LPE and 18:0 LPE. Noteworthy, inhibitor of Gq/11 protein inhibited 16:0 LPE-stimulated neurite outgrowth but not 18:0 LPE-stimulated neurite outgrowth. In contrast, inhibitor of Gi/Go proteins inhibited 18:0 LPE-stimulated neurite outgrowth but not 16:0 LPE-stimulated neurite outgrowth. The effect of PKC inhibitors on neurite outgrowth was also different. (**Chapter 2-3-6**).

Collectively, these results suggest that the structurally different LPE species, 16:0 LPE and 18:0 LPE stimulate neurite outgrowth through distinct signaling cascades in cultured cortical neurons and that distinct G protein-coupled receptors are involved in these processes.

Next, liquid chromatography-electrospray ionization tandem mass spectrometry analysis (LC-ESI-MS/MS) was performed to examine the composition of LPE molecular species in the mouse brain (**Chapter 3-3-1**). Among major LPE species in brain, I examined the roles of oleoyl-LPE (18:1 LPE), that has mono-unsaturated fatty acid chain.

In cultured cortical neurons, 18:1 LPE stimulated neurite outgrowth (**Chapter 3-3-2**). Then, using several G-proteins and enzyme inhibitors, I examined whether the G protein-coupled receptors and its downstream signals are involved in the actions of 18:1 LPE. Inhibitor of Gq/11 protein inhibited 18:1 LPE-stimulated neurite outgrowth. The application of PLC inhibitor, PKC inhibitor, or MAPK inhibitor inhibited 18:1 LPE-stimulated neurite outgrowth. These inhibitor experiments suggest that the effect of 18:1 LPE on neurite outgrowth is mediated by GPCR-activated Gq/11 protein and its downstream PLC/PKC/MAPK (**Chapter 3-3-3**). Western blot analysis showed that 18:1 LPE activates MAPK (**Chapter 3-3-4**). Moreover, I found that 18:1 LPE protects cultured cortical neurons against glutamate-induced excitotoxicity, and involvement of PKC inhibitor Go6983-sensitive PKC subtype in this protective effect of 18:1 LPE (**Chapter 3-3-5**). To my best knowledge, this is the first report showing the protective effect of LPE on glutamate toxicity.

Collectively, these results demonstrate that 18:1 LPE, one of abundant LPE species in brain, exerts the stimulation of neurite outgrowth and protection against glutamate-induced excitotoxicity in cultured cortical neurons.

Chapter 2

Structurally different lysophosphatidylethanolamine species stimulate neurite outgrowth in cultured cortical neurons via distinct G-protein-coupled receptors and signaling cascades

2-1 Abstract

Neurite outgrowth is important in neuronal circuit formation and functions, and for regeneration of neuronal networks following trauma and disease in the brain. Thus, identification and characterization of the molecules that regulate neurite outgrowth are essential for understanding how brain circuits form and function and for the development of treatment of neurological disorders. In this study, I found that structurally different lysophosphatidylethanolamine (LPE) species, palmitoyl-LPE (16:0 LPE) and stearoyl-LPE (18:0 LPE), stimulate neurite growth in cultured cortical neurons. Interestingly, YM-254890, an inhibitor of Gq/11 protein, inhibited 16:0 LPE-stimulated neurite outgrowth but not 18:0 LPE-stimulated neurite outgrowth. In contrast, pertussis toxin, an inhibitor of Gi/Go proteins, inhibited 18:0 LPE-stimulated neurite outgrowth but not 16:0 LPE-stimulated neurite outgrowth. The effects of protein kinase C inhibitors on neurite outgrowth were also different. In addition, both 16:0 LPE and 18:0 LPE activate mitogen-activated protein kinase (MAPK)/extracellular signal-regulated kinase (ERK)1/2, but the effect of the MAPK inhibitor differed between the 16:0 LPE- and 18:0 LPE-treated cultures. Collectively, the results suggest that the structurally different LPE species, 16:0 LPE and 18:0 LPE stimulate neurite outgrowth through distinct signaling cascades in cultured cortical neurons and that distinct G protein-coupled receptors are involved in these processes.

2-2 Introduction

Neurite outgrowth is important in neuronal wiring during development and synaptic plasticity under physiological conditions, and in the regeneration of neuronal wiring following trauma and disease in the brain [**1–4**]. Thus, identifying the molecules that regulate neurite outgrowth and elucidating their mechanism are essential for understanding of mechanisms of neuronal wiring and brain functions, and for development of therapeutics to treat trauma or neurological disorders. To date, several extracellular ligands that regulate the neurite outgrowth of central nervous system (CNS) neurons have been identified. These ligands are varied and include neurotrophins, Wnt proteins, neurotransmitters, neuropeptides, and hormones [**5–11**].

Phospholipids are amphiphilic molecules with a hydrophilic head esterified by a hydrophobic fatty acid chain. They play crucial roles in various biological processes, ranging from structural integrity of cellular and organelle membranes to intracellular signal transduction [**20**]. The brain is one of the most lipid-rich organs, and phospholipids especially play important roles not only in membrane organization but also in brain function [**3**, **13**, **23**]. Among the physiologically active phospholipids, the role of lysophospholipids in biological functions has attracted recent attention. Lysophospholipids consist of a hydrophilic head group and one hydrophobic fatty acid chain, and many lysophospholipid molecular species exist. Lysophosphatidylethanolamine (LPE) is one of the lysophospholipids derived from phosphatidylethanolamine (PE) via a phospholipase A-type reaction and is known to be a minor constituent of cell membranes [**22**, **31**]. As for other lysophospholipids, LPE presents many structurally different species that differ in fatty acid length and degree of unsaturation [**31**]. Extracellularly, LPE has been detected in human serum at levels of several hundred nanograms per milliliter [**32**], but its physiological role remains largely unknown. A few studies suggest the cell-type specific roles of LPE in cultures [**33–36**]. Interestingly, several studies show that cognitive impairment or traumatic brain damage in rodent models is accompanied by changes in LPE revels in the brain [**27**, **29**, **37**]. These suggest the physiological or pathological significance of LPE in the brain. However, to date, the role of LPE in CNS

neurons remains unclear.

In this study, I demonstrate that both palmitoyl LPE (16:0 LPE) and stearoyl LPE (18:0 LPE) stimulate neurite outgrowth in the cultured cortical neurons. Moreover, using several G-proteins and enzyme inhibitors, I found that distinct G-protein-coupled receptors (GPCRs) and signaling cascades are involved in 16:0 LPE and 18:0 LPE-induced neurite outgrowth.

2-3 Result

2-3-1 Effects of phospholipids on neuronal morphology

To examine the effects of phospholipids on neuronal morphology, a commercially available phospholipid kit containing 10 different phospholipids (see the Methods for detail) was applied to cultured cortical neurons prepared form mice embryos. The phospholipids bovine liver lysophosphatidylcholine (LPC), egg yolk LPE, soybean phosphatidylinositol (PI), bovine heart sphingomyelin (SM), porcine brain phosphatidylserine (PS), bovine heart phosphatidylcholine (PC), egg yolk phosphatidylethanolamine (PE), bovine heart cardiolipin (CL), phosphatidic acid (PA) prepared from egg yolk PC, and porcine brain cerebrosides (CB) were applied to a cultured medium at days in vitro (DIV) 3. The cultures were incubated with 1 μM of indicated phospholipids for 11 days, and immunostained with antibodies against MAP2, tau, and NeuN at DIV14, respectively (**Fig. 5**).

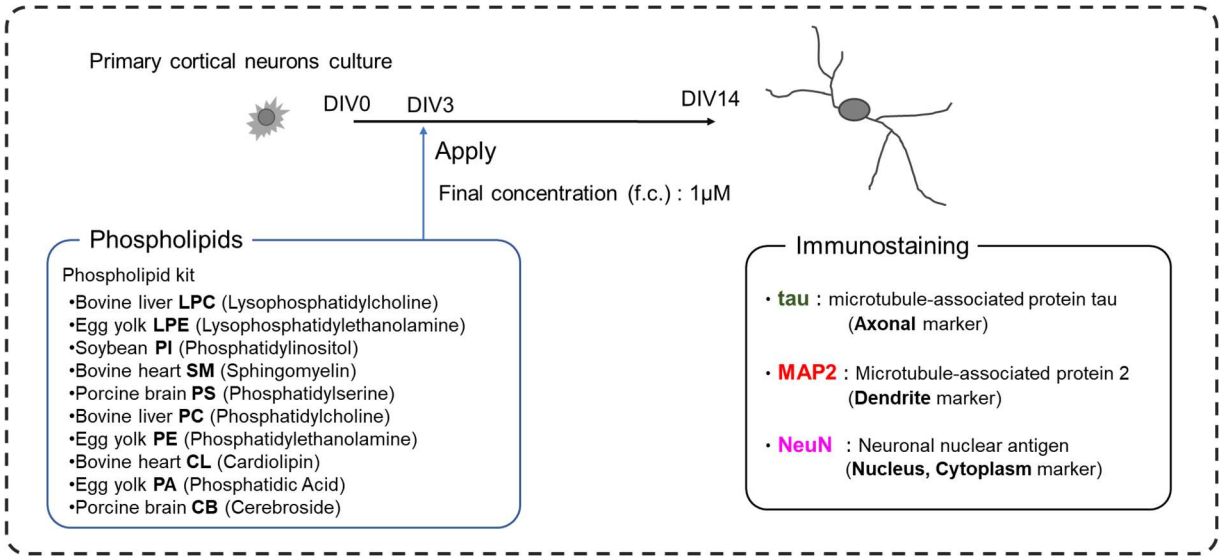

Fig.5 Schematic overview of the experiment on effects of phospholipids on neuronal morphology.

At DIV14, microtubule-associated protein 2 (MAP2)-positive dendrites and microtubule-associated protein tau (tau)-positive axons had spread all over the dish in the control cultures (**Fig. 6A**). When the cultured cortical neurons were incubated with 1 μM egg yolk LPE for 11 days, the tau and MAP2 signals area were significantly increased compared to those in the control cultures (**Fig. 6A–C**). These results suggest that egg yolk LPE strongly stimulates both axonal and dendritic outgrowth in cultured cortical neurons. In cultures treated with soybean PI and bovine heart PC, MAP2 and tau signals were slightly increased compared to those in the control cultures. On the other hand, there was no substantial difference in the number of neuronal nuclear antigen (NeuN)-positive neurons between the control and the cultures treated with phospholipids, except for treatment with bovine heart CL (**Fig. 6A and D**). In the bovine heart CL-treated cultures, the number of NeuN-positive neurons, and the tau and MAP2 signal areas were significantly decreased.

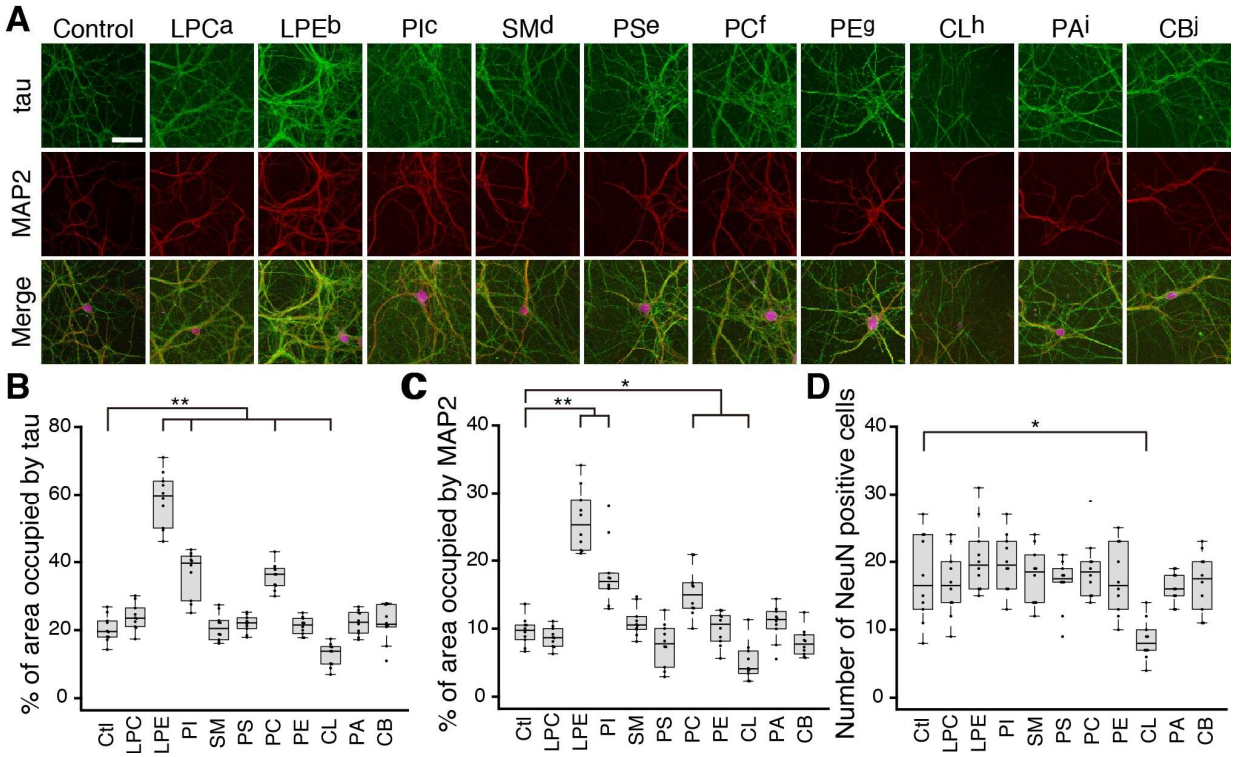

Fig.6 Effects of phospholipids on neuronal morphology. (**A**) Extracellular application of LPE, PI, or PC increased the MAP2 and tau staining signals in the cultured cortical neurons. Scale bar represents 50 μm. [a]bovine liver LPC; [b]egg yolk LPE; [c]soybean PI; [d]bovine heart SM; [e]porcine brain PS; [f]bovine liver PC; [g]egg yolk PE; [h]bovine heart CL; [i]PA form egg yolk PC; [j]porcine brain CB. At DIV3, 1 μM of indicated phospholipids were applied to the culture medium, followed by fixed with 4% paraformaldehyde/4% sucrose at DIV14. (**B**) Quantification of tau signal area in (A). The percentage of tau signal occupied in in the observation field was measured. (**C**) Quantification of MAP2 signal area in (A). The percentage of MAP2 signal occupied in in the observation field was measured. (**D**) Quantification of number of NeuN positive neurons in (A). The horizontal line in each box indicates the median, the box shows the interquartile range (IQR), and the whiskers are 1.5× IQR. Statistical significance was evaluated with the Kruskal–Wallis test followed by post hoc Steel test: ** $p < 0.01$ and * $p < 0.05$, n = 10 areas.

2-3-2 Effects of 16:0 LPE and 18:0 LPE on neuronal morphology

Among phospholipids tested, egg yolk LPE was the most effective on the morphological change. To my knowledge, no previous study has examined the role of LPE in the CNS neurons. Therefore, LPE effects were examined in this study. The LPE used was derived from egg yolk and contained two structurally different LPE species, 16:0 LPE and 18:0 LPE. To examine whether 16:0 LPE or 18:0 LPE effects the neuronal morphology, cultured cortical neurons were incubated with different concentrations of LPE, 16:0 LPE, and 18:0 LPE for 11 days and immunostained with antibodies against MAP2, tau, and NeuN at DIV14, respectively (**Fig. 7**).

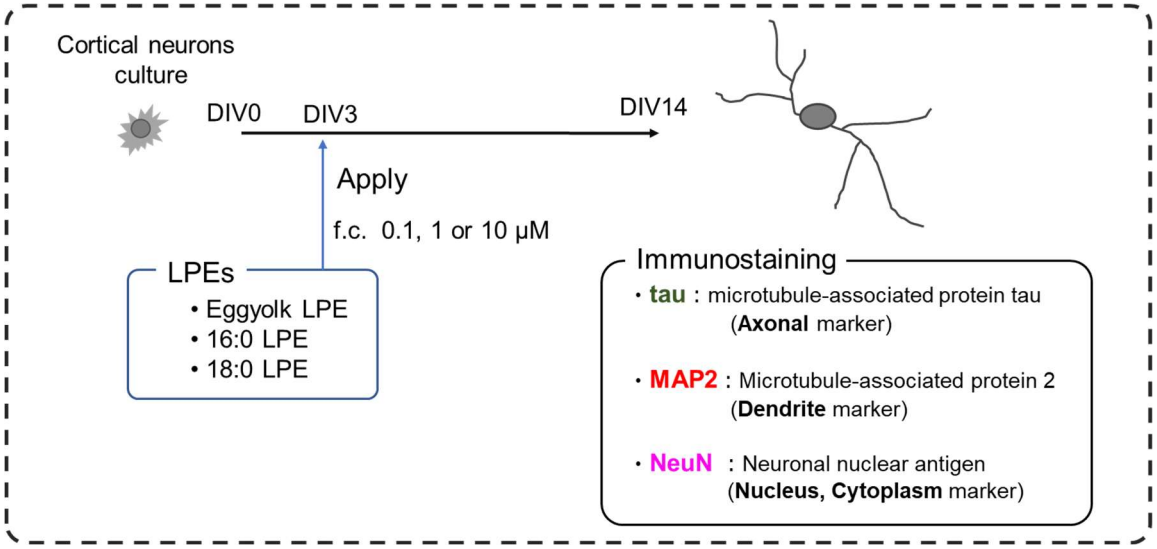

Fig.7 Schematic overview of an experiment on effects of LPEs on neuronal morphology.

Incubation with 0.1 or 1 μM 16:0 LPE significantly increased the tau and MAP2 signal areas compared to those in the control cultures (**Fig. 8A–C**). At a higher concentration of 10 μM, 16:0 LPE did not significantly increase these signal areas. On the other hand, 18:0 LPE significantly increased the tau and MAP2 signal areas at all concentrations (**Fig. 8A–C**). There was no substantial difference in the number of NeuN-positive neurons when comparing the control and the LPEs-treated cultures (**Fig. 8A and D**). These results suggest that the structurally distinct LPE species 16:0 LPE and 18:0 LPE both increase axonal and dendritic area in cultured cortical neurons.

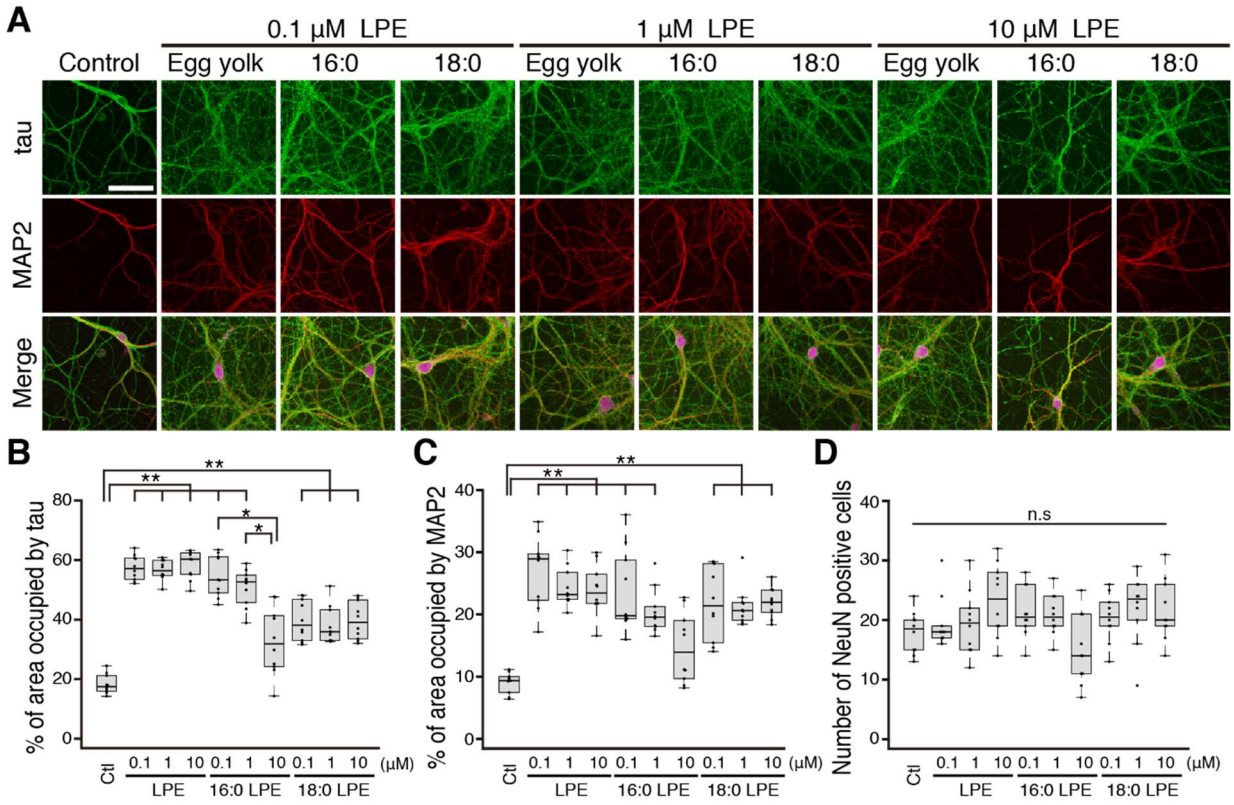

Fig. 8 Effects of 16:0 LPE and 18:0 LPE on neuronal morphology.

(**A**) Extracellular application of 16:0 LPE and 18:0 LPE increased the MAP2 and tau staining signals in the cultured cortical neurons. Scale bar represents 50 μm. (**B**) Quantification of tau signal area in (A). The percentage of tau signal occupied in in the observation field was measured. (**C**) Quantification of MAP2 signal area in (A). The percentage of MAP2 signal occupied in in the observation field was measured. (**D**) Quantification of number of NeuN positive neurons in (A). The horizontal line in each box indicates the median, the box shows the IQR, and the whiskers are 1.5× IQR. Statistical significance was evaluated with the Kruskal–Wallis test followed by post hoc Steel–Dwass test: ** $p < 0.01$, * $p < 0.05$, n = 10 areas.

2-3-3 Effects of 16:0 LPE and 18:0 LPE on neurite outgrowth

The effects of 16:0 LPE and 18:0 LPE on neurite outgrowth were examined by directly measuring the length of neurites. Either 16:0 LPE or 18:0 LPE was applied at 1 μM to the culture medium at DIV0, and the neurites were measured at DIV1, 2, and 3, respectively (**Fig. 9**).

From DIV0 to DIV3, the lengths of neurites were gradually increased in all conditions. In cultures treated with 16:0 LPE and 18:0 LPE, the neurites were significantly longer than those of control cultures (**Fig. 10A and B**). The number of neurites emerging from the soma was also increased in these cultures at DIV1 and 2 (**Fig. 10A and C**). On the other hand, the numbers of branches for the longest neurite in 16:0 LPE- and 18:0 LPE-treated cultures were comparable to those in the control culture (**Fig. 10A and D**). In terms of morphologies examined, there was no substantial difference between the 16:0 LPE- and 18:0 LPE-treated cultures.

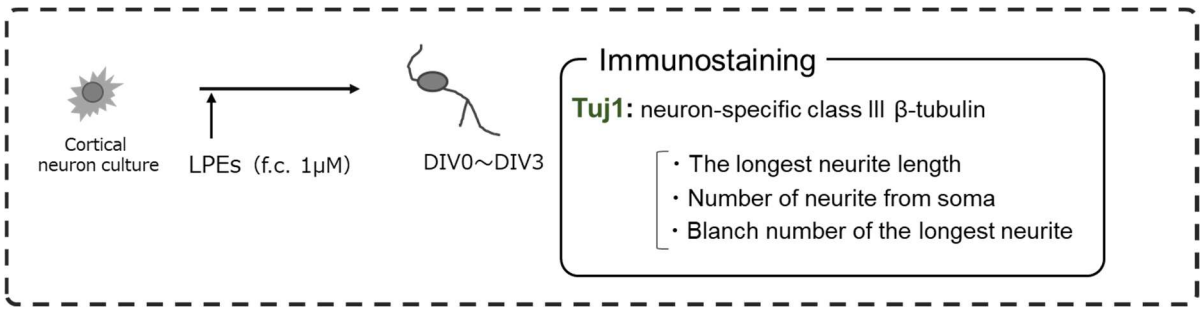

Fig.9 Schematic overview of the experiment on effects of LPEs on neurite outgrowth.

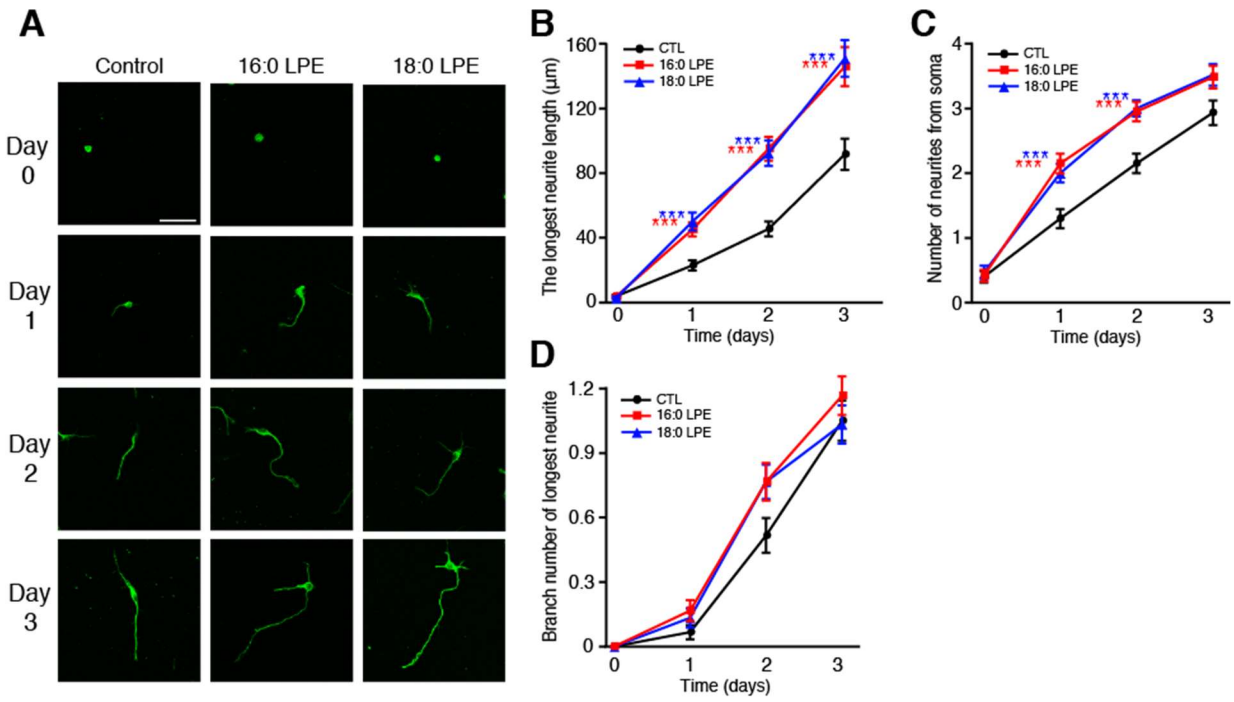

Fig. 10 Effects of 16:0 LPE and 18:0 LPE on neurite outgrowth.

(**A**) Extracellular application of 16:0 LPE and 18:0 LPE stimulates neurite outgrowth of the cultured cortical neurons. Scale bar represents 50 μm. (**B**) Quantification of the length of the longest neurite emerging from the soma was measured in (A). (**C**) Quantification of the number of neurites emerging from the soma in (A). (**D**) Quantification of the numbers of branches per longest neurite in (A). All values represent mean ± s.e.m. Statistical significance was evaluated Kruskal–Wallis test followed by post hoc Steel–Dwass test: *** $p < 0.001$, n = 60 cells.

The effects of different concentrations of 16:0 LPE and 18:0 LPE were also examined in terms of neurite outgrowth. The cultured cortical neurons were incubated with 0.5 μM to 10 μM 16:0 LPE or 18:0 LPE, and the length of the longest neurites was measured at DIV3. Both 16:0 LPE and 18:0 LPE dose-dependently increased the length of neurites (**Fig. 11A and B**). At a concentration of 10 μM, both LPEs increased the neurite length to approximately twice as long as that in the control cultures. There was no significant difference between 16:0 LPE and 18:0 LPE in the lengths at any concentration. These results suggest that 16:0 LPE and 18:0 LPE stimulate neurite outgrowth in cultured cortical neurons and have similar effects on neuronal morphology.

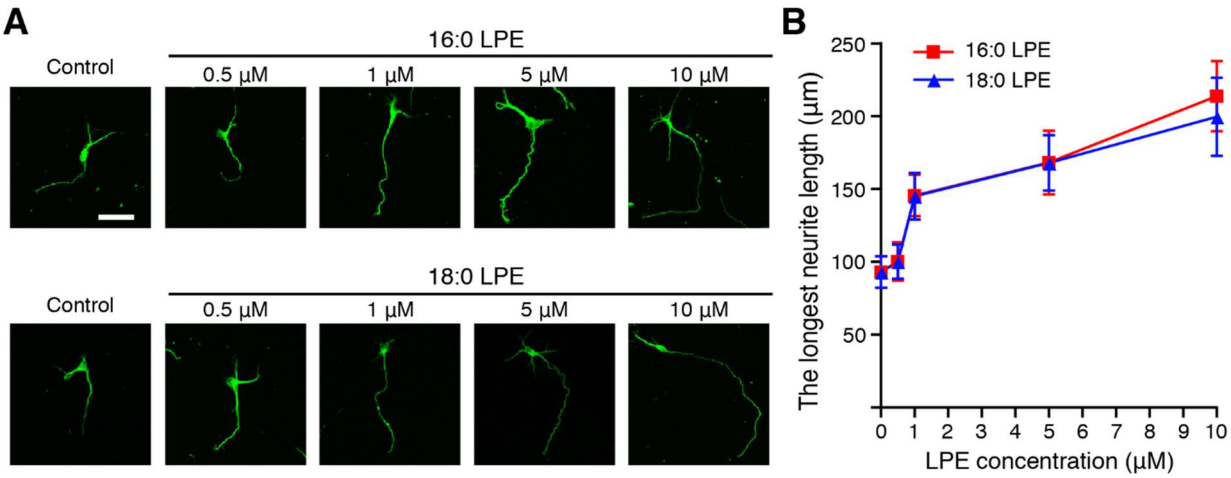

Fig.11 Dose-dependent stimulation of neurite outgrowth by application of 16:0 LPE and 18:0 LPE.

(**A**) Applied 16:0 LPE and 18:0 LPE stimulate neurite outgrowth of cultured cortical neurons in a dose dependent manner. Indicated concentration of 16:0 LPE or 18:0 LPE was applied to the cultures at DIV0, and immunostained with antibody against Tuj1 at DIV3, respectively. Scale bar represents 50 μm. (**B**) Quantification of the length of the longest neurite in (A). Red-filled squares and blue-filled triangles represent 16:0 LPE-treatment and 18:0 LPE-treatment cultures, respectively. All values represent mean ± s.e.m. Statistical significance was evaluated using two-way ANOVA, n = 20 cells.

2-3-4 LPEs activate MAPK in cultured cortical neurons.

It has been reported that LPE activates MAPK/ERK 1/2 in manner that depends on cell type [**33**, **35**, **38**, **39**]. However, the response of LPE in neurons remains unknown. It is known that MAPK signal cascade involved in neurite outgrowth [**40**]. Thus, one possibility is that 16:0 LPE and 18:0 LPE activate MAPK/ERK1/2 in the cultured cortical neurons. To examine whether this takes place, the cultured cortical neurons were incubated with 16:0 LPE or 18:0 LPE for 10 min and subjected to western blot analysis using anti-phospho-ERK1/2 and anti-ERK1/2 antibodies (**Fig. 12**).

Anti-ERK1/2 antibody then detected the bands corresponding to the size of ERK1/2 in all conditions (**Fig. 13A**). In the absence of LPE, anti-phospho-ERK1/2 antibody detected bands corresponding to the size of phosphorylated ERK1/2, and incubation of 16:0 LPE and 18:0 LPE significantly increased those signals in a dose-dependent manner (**Fig. 13A, B**). These results suggest that both 16:0 LPE and 18:0 LPE activate MAPK/ERK1/2 in cultured cortical neurons.

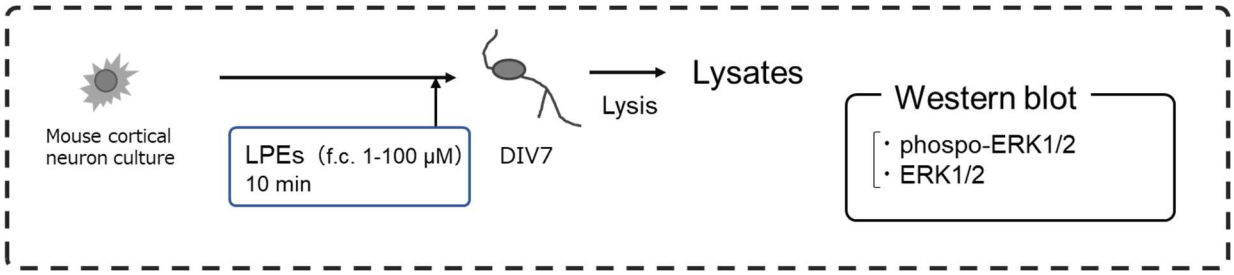

Fig. 12 Schematic overview of the experiment on western blot analysis.

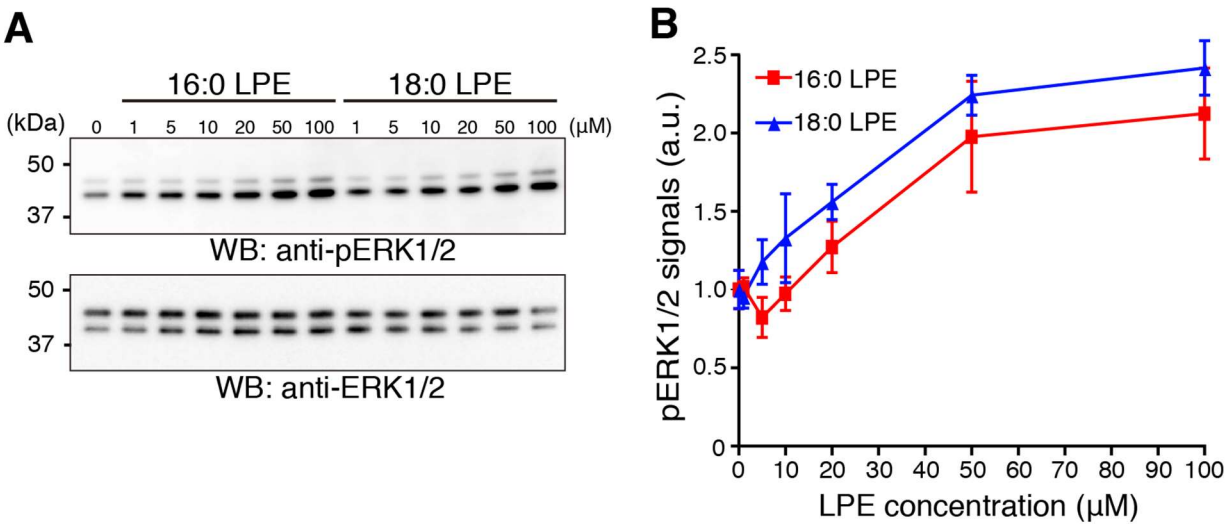

Fig. 13 Effects of 16:0 LPE and 18:0 LPE on activation of MAPK in cultured cortical neurons. (**A**) 16:0 LPE and 18:0 LPE induce the phosphorylation of MAPK/ERK1/2. At DIV7, the cultures were incubated with indicated concentrations of 16:0 LPE or 18:0 LPE for 10 min. Lysates were subjected to SDS-PAGE, followed by Western blot analysis using anti-phospo-ERK1/2 and anti-ERK1/2 antibodies. (**B**) Quantification of phosphorylated ERK1/2 signals in (A). Intensities of phosphorylated ERK1/2 signals were normalized with those of ERK1/2 signals. Red-filled squares and blue-filled triangles represent 16:0 LPE-treatment and 18:0 LPE-treatment cultures, respectively. All values represent mean ± s.e.m. Statistical significance was evaluated using two-way ANOVA followed by *post hoc* Student's t test. n = 3 cultures.

2-3-5 Effects of MAPK inhibitor on LPE-stimulated neurite outgrowth

The finding of activation of MAPK/ERK1/2 in 16:0 LPE- and 18:0 LPE-treated cortical cultures rises the possibility that these LPEs stimulate neurite outgrowth through the activation of MAPK/ERK1/2. To examine this, the cultured cortical neurons were treated with MAPK inhibitor U0126 at 5 μM in the presence or absence of 16:0 LPE or 18:0 LPE for 3 days (**Fig. 14**). This concentration of U0126 completely inhibited activation of MAPK/ERK1/2 (**Fig. 15A and B**). In the control cultures at DIV3, application of U0126 significantly decreased the length of neurites. In cultures treated with 18:0 LPE, U0126 significantly decreased the length of neurite to a degree comparable to that in the U0126-treated control cultures (**Fig. 15C and D**). In contrast, U0126 decreased 16:0 LPE-stimulated neurite length, although these were longer than in the control U0126-treated, and 18:0 LPE and U0126-treated cultures. These results suggest that 16:0 LPE and 18:0 LPE stimulate neurite outgrowth through the activation of MAPK. In addition, the differential effect of MAPK inhibitor on 16:0 LPE- and 18:0 LPE-stimulated neurite outgrowth raises the possibility that these LPEs activate distinct membrane receptors and signaling cascades.

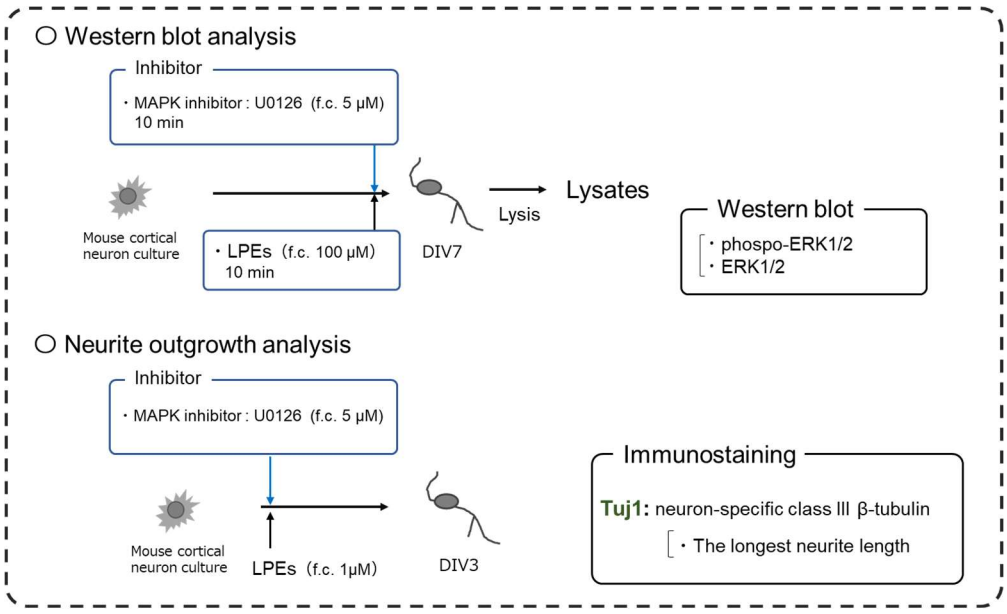

Fig. 14 Schematic overview of the experiment on effects of MAPK inhibitor U0126 on 16:0 LPE- and 18:0 LPE-stimulated neurite outgrowth.

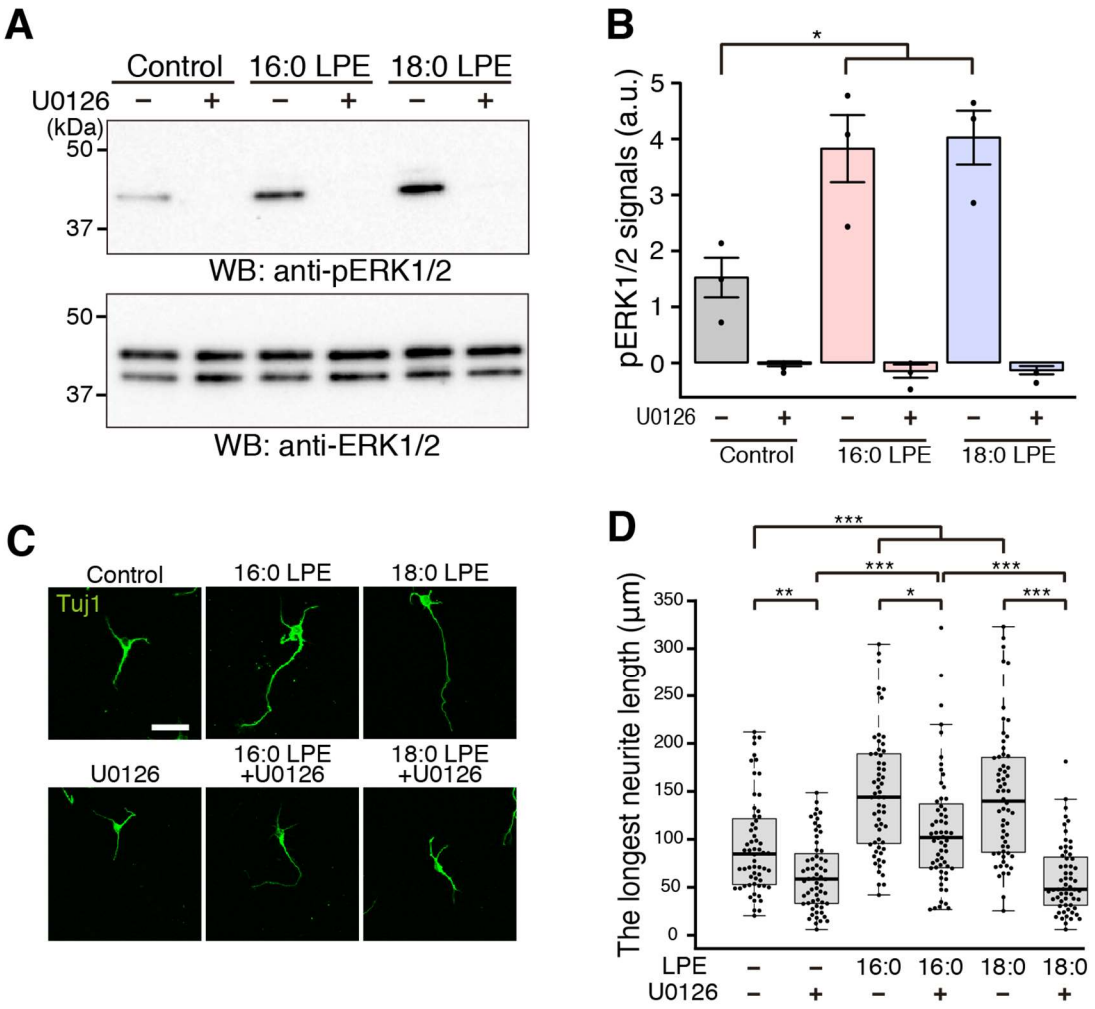

Fig. 15 Effects of MAPK inhibitor U0126 on 16:0 LPE- and 18:0 LPE-stimulated neurite outgrowth.

(**A**) U0126 inhibits 16:0 LPE or 18:0 LPE-induced phosphorylation of ERK1/2. (**B**) Quantification of phosphorylated ERK1/2 signals in (A). Intensities of phosphorylated ERK1/2 signals were normalized with those of ERK1/2 signals. All values represent mean ± s.e.m. (**C**) MAPK inhibitor U0126 inhibited 18:0 LPE-stimulated neurite outgrowth and partially inhibited 16:0 LPE-stimulated neurite outgrowth. Scale bar represents 50 μm. (**D**) Quantification of the length of the longest neurite in (C). The horizontal line in each box indicates the median, the box shows the IQR, and the whiskers are 1.5× IQR. Statistical significance was evaluated with the Kruskal–Wallis test followed by post hoc Steel–Dwass test in (D) or evaluated using one-way ANOVA followed by *post hoc* Tukey's test in (B). *** $p < 0.001$, ** $p < 0.01$, and * $p < 0.05$, n = 60 in (D) and n= 3 in (B), respectively.

2-3-6 Effects of G-protein and enzyme inhibitors on LPE-stimulated neurite outgrowth

Several studies suggest that the one of actions of LPE is mediated by G-protein-coupled receptor (GPCR)-activated phospholipase C (PLC) [**34**, **35**, **41–43**]. To examine whether the GPCR-PLC cascade mediates the actions of 16:0 LPE and 18:0 LPE, cultured cortical neurons were incubated with Gq/11 inhibitor YM-254890 or Gi/Go inhibitor pertussis toxin (PTX) (**Fig. 16**). Application of YM-254890 decreased the length of 16:0 LPE-stimulated neurite, but not that of 18:0 LPE-stimulated neurite (**Fig. 17A and D**). In contrast, PTX decreased the length of 18:0 LPE-stimulated neurite, but not that of 16:0 LPE-stimulated neurite (**Fig. 17B and E**). PLC inhibitor U73122 decreased both the length of 16:0 LPE- and 18:0 LPE-stimulated neurite (**Fig. 17C and F**).

It is known that activation of PLC leads to production of inositol 1,4,5-tri-sphosphate and diacylglycerol, the activator for PKC. To examine whether PKC is involved in LPEs-stimulated neurite outgrowth, the PKC inhibitor Go6983, which inhibits PKCα, β, γ, δ, and ζ [**44**], was applied to the cultures. Application of 1 μM Go6983 inhibited 18:0 LPE-stimulated neurite outgrowth. In contrast, Go6983 had little effect on 16:0 LPE-treated cultures (**Fig. 18A, C**). It is known that PKC family proteins consist of PKCα, β, γ, δ, ε, η, θ, ζ, Mζ, and ι/λ [**45**]. Therefore, a different PKC inhibitor, Sotrastaurin, which inhibits PKCα, β, δ, ε, η, and θ [**46**], was selected. When Sotrastaurin was applied to the cultures, both 16:0 LPE- and 18:0 LPE-stimulated neurite length changes were completely inhibited (**Fig. 18B, D**). These results suggest that 16:0 LPE and 18:0 LPE activate distinct receptors and signaling cascades involved in the neurite outgrowth.

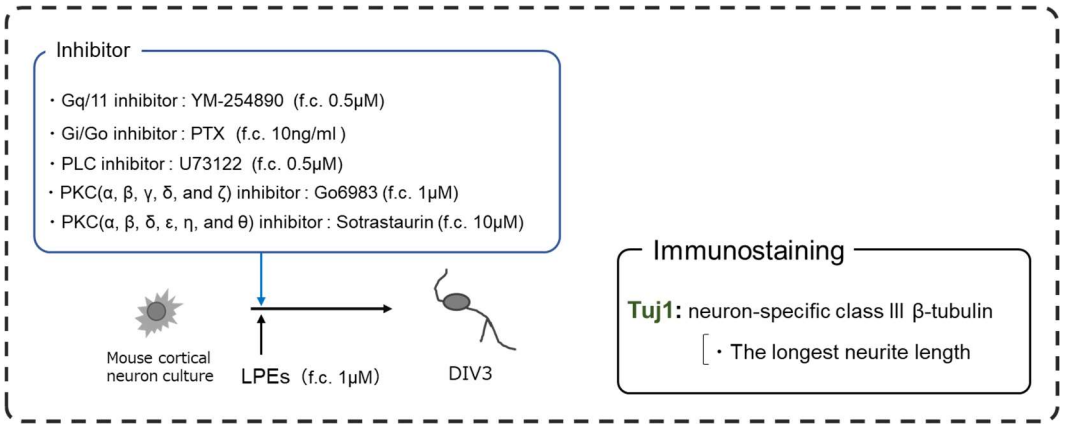

Fig. 16 Schematic overview of the experiment on effects of G-proteins and enzyme inhibitors on 16:0 LPE and 18:0 LPE-stimulated neurite outgrowth.

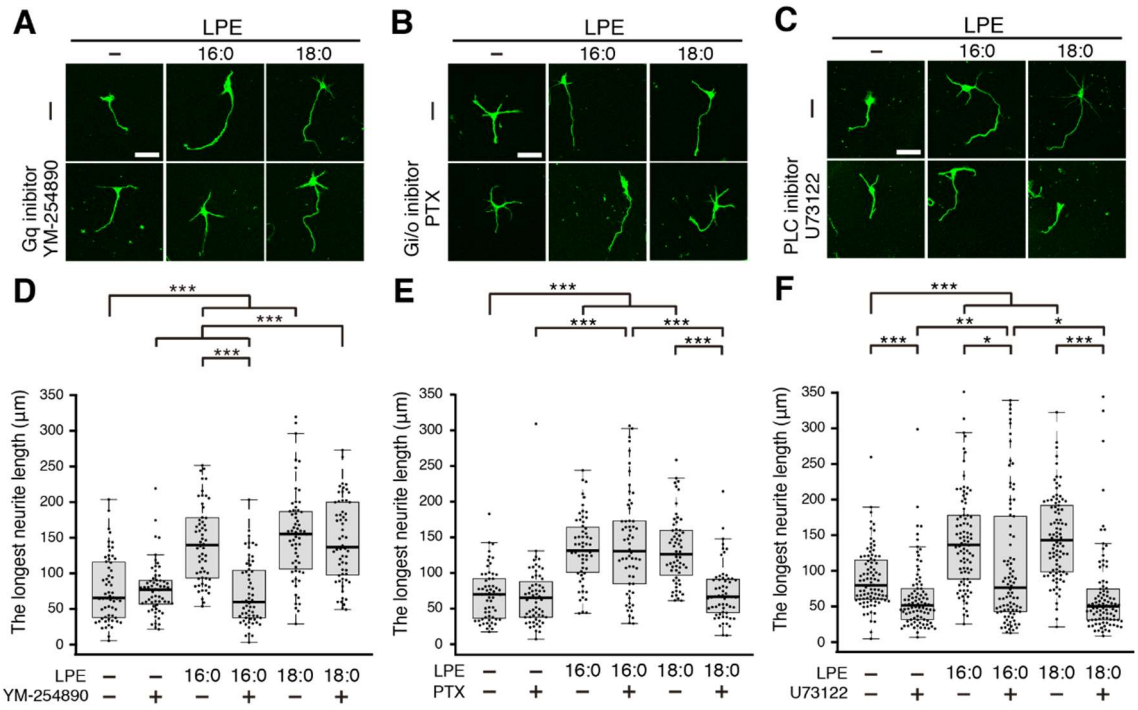

Fig. 17 Effects of inhibitors for G-proteins and PLC on 16:0 LPE- and 18:0 LPE-stimulated neurite outgrowth. (**A–C**) Effects of Gq/11 inhibitor YM-254890 (**A**), Gi/Go inhibitor PTX (**B**), PLC inhibitor U73122 (**C**) on 16:0 LPE- and 18:0 LPE-stimulated neurite outgrowth. (**D–F**) Quantification of the length of the longest neurite in (A–C). Scale bars represent 50 μm in (A–C). The horizontal line in each box indicates the median, the box shows the IQR, and the whiskers are 1.5× IQR. Statistical significance was evaluated with the Kruskal–Wallis test followed by post hoc Steel–Dwass test: *** $p < 0.001$, ** $p < 0.01$, * $p < 0.05$, n = 60 cells in (D and E), n = 90 cells in (F).

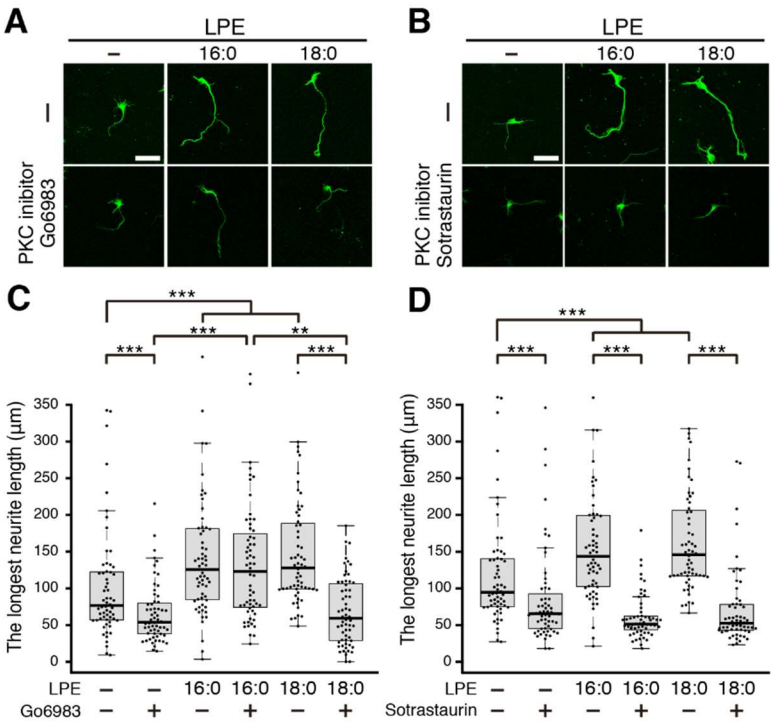

Fig. 18 Effects of PKC inhibitors on 16:0 LPE- and 18:0 LPE-stimulated neurite outgrowth.

(**A**) Effects of PKC inhibitor Go6983 on 16:0 LPE- and 18:0 LPE-stimulated neurite outgrowth.

(**B**) Effects of PKC inhibitor Sotrastaurin on 16:0 LPE- and 18:0 LPE-stimulated neurite outgrowth.

(**C and D**) Quantification of the length of the longest neurite in (A and B). Scale bars represent 50 μm in (A and B). The horizontal line in each box indicates the median, the box shows the IQR, and the whiskers are 1.5× IQR. Statistical significance was evaluated with the Kruskal–Wallis test followed by post hoc Steel–Dwass test: *** $p < 0.001$, ** $p < 0.01$, n = 60 cells in (C and D).

2-4 Discussion

Recent attention has focused on the role of lysophospholipids in biological functions. However, in the CNS neurons, the cellular response to extracellular lysophospholipids remains largely unclear, although some phospholipids such as lysophosphatidic acid (LPA), sphingosine-1-phosphate (S1P), and 2-arachidonoylglycerol have been reported to act extracellularly as an agonist on their membrane receptor and to regulate neuronal functions [**24**, **25**, **26**, **48**]. In this study, I found that extracellular application of 16:0 LPE and 18:0 LPE stimulates neurite outgrowth in cultured cortical neurons. In addition, I found the involvement of distinct GPCRs and signaling cascades in 16:0 LPE and 18:0 LPE-induced neurite outgrowth.

The effects of 16:0 LPE and 18:0 LPE in stimulating neurite outgrowth in cultured cortical neurons are clearly shown (**Fig. 10 and 11**). LPE is a minor constituent of cell membranes [**31**]. Extracellularly, LPE was detected in human serum in the range of several hundred nanograms per milliliter [**32**], but its physiological role remains largely unknown. A few studies have indicated roles for LPE in culture cells, as follows: The LPE extracted from *Grifola frondosa*, a kind of mushroom, stimulates neurite-like outgrowth of rat pheochromocytoma PC12 cells [**33**]. The 18:1 LPE stimulates chemotactic migration and cellular invasion in SK-OV3 human ovarian cancer cells [**34**] and cell proliferation of MDA-MB-231 breast cancer cells [**35**]. Egg yolk LPE stimulates differentiation and maturation of mouse astrocyte in culture [**36**]. Thus, LPE evokes various responses, depending on the cell type. At this time, whether LPE promotes neurite outgrowth in other types of CNS neurons remains unclear.

In cultured cortical neurons, 16:0 LPE-stimulated neurite outgrowth was inhibited by Gq/11 inhibitor YM-254890 and PLC inhibitor U73122 (**Fig. 17**), suggesting that the action of 16:0 LPE is mediated by Gq/11-coupled GPCR activated PLC. On the other hand, 18:0 LPE-stimulated neurite outgrowth was inhibited by Gi/Go inhibitor PTX and U73122 (**Fig. 17**), suggesting that the action of 18:0 LPE is mediated Gi/Go-coupled GPCR activated PLC [**49**]. Thus, different types of GPCRs are likely to exist

for 16:0 LPE and 18:0 LPE. In addition to neurite outgrowth, 16:0 LPE and 18:0 LPE may have different physiological functions for cortical neurons. Further investigation is needed to clarify this.

To date, receptors for LPE remains unidentified, but several studies have suggested the existence of cell type-specific GPCRs for different LPE species [**34**, **35**, **41–43**]. For example, in MDA-MB-231cells, 18:1 LPE stimulates intracellular Ca^{2+} concentration, and this effect is inhibited by PTX or LPA receptor LPA_1 antagonist AM095 [**34**, **41**]. On the other hand, in SK-OV3 cells, the effect of 18:1 LPE-stimulated intracellular Ca^{2+} concentration is inhibited by PTX, but not by AM095 [**34**, **35**]. In addition, in some cells, LPE stimulates intracellular Ca^{2+} concentration, but their effect is completely dependent on the fatty acid lengths of the LPE [**34**, **35**, **41–43**]. For example, in PC12 cells, intracellular Ca^{2+} concentration is stimulated by 18:0 LPE and 14:0 LPE, but not 16:0 LPE [**42**]. Identification of receptors for 16:0 LPE and 18:0 LPE will be needed to completely elucidate how LPE induces a signal cascade in the cortical neuron.

Many ligands including neurotrophins, Wnt proteins, neurotransmitters, hormones, and neuropeptides have been identified as stimulating neurite outgrowth of neurons via binding to their receptors [**5**–**11**], and diverse protein kinase signal cascades including MAPK and PKC are involved in this process [**40**]. In the cultured cortical neurons, extracellular application of both 16:0 LPE and 18:0 LPE activated MAPK/ERK1/2 (**Fig. 13**). It has reported that 14:0 LPE, 16:0 LPE, and 18:1 LPE activate MAPK/ERK1/2 in PC12 cells [**33**] and 18:1 LPE activates ERK1/2 in human MDA-MB-231 breast cancer cell line [**35**]. LPE, although not reported in terms of specific type, did not activate MAPK in murine mesangial cells [**39**]. However, for PC12 cells, contrary to the observations noted by Nishina et al. [**33**], there is a report that 16:0 LPE does not activate MAPK/ERK1/2 in these cells [**38**]. These previous studies suggest the existence of a cell-type dependent MAPK activation mechanism for LPE. Interestingly, in cultured cortical neurons, inhibition of MAPK inhibited 18:0 LPE-stimulated neurite outgrowth and partially inhibited 16:0 LPE-stimulated neurite outgrowth (**Fig. 15**). In addition, Sotrastaurin, which inhibits PKCα, β, δ, ε, η, and θ [**46**], inhibited both 16:0 LPE- and 18:0 LPE-induced

neurite outgrowth. In contrast, Go6983, which inhibits α, β, γ, δ, and ζ [**44**], inhibited the effect of 18:0 LPE but not the effect of 16:0 LPE (**Fig. 18**). Combining these results with the PLC inhibitor results (**Fig. 17**), suggests that 16:0 LPE and 18:0 LPE stimulate neurite outgrowth in the cortical neurons through different receptors and signaling pathways.

Thus far, the roles of LPE in the brain have not been clarified, but several reports suggest the pathophysiological significance of LPE. Previous reports show that cognitive impairment or traumatic brain damage is associated with an imbalance in the composition of phospholipids in the brain. Aged triple transgenic Alzheimer's model mice harboring $PS1_{M146V}$, APP_{Swe}, and tau_{P301L} transgenes with cognitive impairment show increasement of LPE in the hippocampus [**37**, **50**]. Postischemic cognitive impairment rat model shows increasement of LPE species, 18:1, 20:3, and 22:6 LPE, in the hippocampus [**27**]. Traumatic brain injury in rat transiently increases 22:6 LPE in the injury area [**29**]. A change in LPE was reported in the serum of a major depressive disorder patient [**28**]. These observations imply the importance of LPE in the brain in normal development, as well as in pathological settings. Comprehensive analysis of LPE species in the brain and investigation of their functions are necessary to understand their roles in pathophysiological conditions.

2-5 Material and Methods

2-5-1 Cell cultures

Primary cortical neuron cultures were prepared from ICR mice at embryonic day 18 as previously described [**51**]. Briefly, the cerebral cortices were treated with phosphate-buffered saline (PBS) containing 1% trypsin (Sigma-Aldrich) and 0.1% DNase I (Sigma-Aldrich) for 5 min and dissociated by passing through a fire-polished Pasteur pipette in PBS containing 0.05% DNase I, 0.03% trypsin inhibitor (Sigma-Aldrich), and 2 mM $MgCl_2$. The cells were placed on 12mm diameter coverslips coated with 30 μg/ml poly-L-lysine (weight 70–150 kDa; Sigma-Aldrich) and 10 μg/ml mouse laminin (Thermo Fisher Scientific) at a density of 1.0×10^5 cells/well on 24-well culture plates. The cells were maintained in Neurobasal-A (Thermo Fisher Scientific) supplemented with 2% B-27 supplement (Thermo Fisher Scientific), 5% fetal calf serum (FCS), 100 U/ml penicillin, 100 μg/ml streptomycin, and 0.2 mM GlutaMax-I (Thermo Fisher Scientific) for 24 h and then the medium was changed to the same medium without FCS. All animal procedures were approved by the Animal Care and the Use Committee of Shinshu University (Approval No. 290072).

2-5-2 Morphological analysis

Phospholipid kit including bovine liver LPC containing primary C18:0, egg yolk LPE containing primary C16:0 and C18:0, soybean PI containing primary C16:0 and C18:2, bovine heart SM containing primary C16:0, C18:0, and C18:1, porcine brain PS containing primary C18:0 and C18:1, bovine liver PC containing primary C18:0 and C18:1, egg yolk PE containing primary C16:0, C18:0, C18:1, and C18:2, bovine heart CL containing primary C18:2, PA from egg yolk containing primary C16:0 and C18:1, and porcine brain CB containing primary C22:0 and C24:0 were purchased from Olbracht Serdary

Research Laboratories (Toronto, Canada). At DIV3, 1 μM LPC, LPE, PI, PS, PC, PE, CL, PA, and CB was applied to the culture medium, respectively. The cultures were fixed with 4% paraformaldehyde/4% sucrose at DIV14. The fixed cells were incubated with PBS buffer containing 0.25% Triton X-100 for 5 min and immunostained with rabbit anti-MAP2 (1:1000; Sigma-Aldrich), goat anti-tau (1:1000; Santa Cruz Biotechnology), and mouse anti-NeuN (1:500; Merk Millipore) antibodies, followed by incubation with donkey Alexa Fluor 488-conjugated anti-goat IgG (1:500; Thermo Fisher Scientific), donkey Alexa Fluor 555-conjugated anti-rabbit IgG (1:500; Thermo Fisher Scientific), and donkey Alexa Fluor 647-conjugated anti-mouse IgG antibodies (1:500; Thermo Fisher Scientific). 16:0 LPE (Avanti) and 18:0 LPE (Avanti) were used to analyze the effect of the difference in the structure of LPEs. For analysis of the time course of neurite outgrowth, 1 μM 16:0 LPE or 18:0 LPE was applied to the culture medium at DIV0. The cultures were fixed with 4% paraformaldehyde/4% sucrose at DIV1, DIV2, and DIV3, respectively.

For inhibitor experiments, Gi/Go inhibitor PTX (1 ng/ml; Wako Pure Chemical Industries), Gq/11 inhibitor YM-254890 (0.5 μM; Wako Pure Chemical Industries), PLC inhibitor U73122 (0.5 μM; CAYMAN CHEMICAL), MAPK inhibitor U0126 (5 μM; CAYMAN CHEMICAL), PKC inhibitor Sotrastaurin (10 μM; CAYMAN CHEMICAL), or PKC inhibitor Go6983 (1 μM; CAYMAN CHEMICAL) was applied to the culture medium at DIV0, followed by fixed at DIV3 as described above. The fixed cells were treated with 0.25% Triton X-100 for 5 min, and immunostained with mouse anti-Tuj1 (neuron-specific class III β-tubulin, 1:5000; BioLegend), followed by incubation with donkey Alexa Fluor 488-conjugated anti-mouse IgG antibody (1:500; Thermo Fisher Scientific).

2-5-3 Image acquisition and quantification

Images of culture experiments were taken with a confocal laser-scanning microscope (TCS SP8; Leica

Microsystems) using HC PL APO CS2 20×/0.75 NA multiple immersion lens (Leica Microsystems) or HC PL APO CS 10×/0.40 NA multiple immersion lens (Leica Microsystems) under constant conditions in terms of laser power, pinhole size, gain, z-steps, and zoom setting throughout the experiments. All quantitative measurements were performed with ImageJ 1.52a software [**52**]. For the quantification of MAP2 and tau staining areas, z-series of optical sections were projected by the brightest point method. MAP2 and tau staining areas were defined as area in which staining signal intensities were 2 and 3 times stronger than those of background signals on the same field, respectively. For analysis of the time course of neurite outgrowth, z-series of optical sections were projected by the brightest point method. Neurite of cortical neurons was identified by Tuj1 signals, and the length of the longest neurite, the number of neurites emerging from the soma, and the numbers of branches per longest neurite were measured.

2-5-4 Western blot analysis

Primary cortical neuron cultures were prepared as described above and plated on the 24-well dish at a density of 5.0×10^5 cells /well. One to 100 μM 16:0 LPE or 18:0 LPE was applied to the culture medium at DIV7. After 10 min incubation, the cultures were solubilized with SDS sample buffer containing 2% SDS, 50 mM-Tris-HCI, pH6.8, 10% glycerol, 100 mM dithiothreitol, phosphatase inhibitor cocktail (Nakarai Tesque), and 0.025% Bromophenol Blue, followed by boiling at 95℃ for 10 min. For inhibition of MAPK, 5 μM MAPK inhibitor U0126 was applied to the cell culture medium 30 min before treatment with LPE. The cell lysates were separated by SDS-polyacrylamide gel electrophoresis and transferred to PVDF membrane. After blocking with PVDF Blocking Reagent for Can Get Signal (TOYOBO), the membranes were incubated with mouse anti-phospho-MAPK/ERK1/2 (Thr202/Tyr204) antibody (E10, 1:2000; Cell Signaling Technology), followed by incubation with horseradish-peroxidase-conjugated secondary antibody. After stripping, the membranes were probed with rabbit anti p44/42 MAPK antibody

(1:1000; Cell Signaling Technology), followed by incubation with horseradish-peroxidase-conjugated secondary antibody. Can Get Signal Immunoreaction Enhancer Solution (TOYOBO) was used for dilution of antibodies. The proteins were visualized by ECL Select Western Blotting Detection System (GE Healthcare) and detected by Las-4000 mini luminescent imaging analyzer (GE Healthcare). The quantification analysis was performed using ImageQuant TL image analysis software (GE Healthcare).

2-5-5 Statistical analysis

Results of at least two independent experiments were subjected to statistical analyses. No statistical method was used to determine sample size. No data were excluded. There was no randomization of samples before analysis. Statistical significance was evaluated with two-way or one-way ANOVA followed by Tukey's, Dunnett's *post hoc* test, or Student's t-test was used for parametric data analysis. Kruskal–Wallis test followed by post-hoc Steel–Dwass or Steel's test was used for non-parametric data analysis. All statistical analysis using R software (R Core Team, 2017). Statistical significance was assumed when $p < 0.05$.

Chapter 3

Abundant oleoyl-lysophosphatidylethanolamine in brain stimulates neurite outgrowth and protects against glutamate toxicity in cultured cortical neurons

3-1 Abstract

Lysophosphatidylethanolamines (LPEs) are bioactive lysophospholipids that have been suggested to play important roles in several biological processes. In this study, I performed a quantitative analysis of LPE species and showed their composition in mouse brain. I examined the roles of oleoyl-LPE (18:1 LPE), which is one of the abundant LPE species in brain. In cultured cortical neurons, application of 18:1 LPE stimulated neurite outgrowth. The effect of 18:1 LPE on neurite outgrowth was inhibited by Gq/11 inhibitor YM-254890, phospholipase C (PLC) inhibitor U73122, protein kinase C (PKC) inhibitor Go6983, or mitogen-activated protein kinase (MAPK) inhibitor U0126. In addition, 18:1 LPE increased the phosphorylation of MAPK/extracellular signal-regulated kinase 1/2. These results suggest that the action of 18:1 LPE on neurite outgrowth is mediated by the Gq/11/PLC/PKC/MAPK pathway. Moreover, I found that application of 18:1 LPE protects neurons from glutamate-induced excitotoxicity. This effect of 18:1 LPE was suppressed by the PKC inhibitor Go6983. These results suggest that 18:1 LPE protects neurons from glutamate toxicity via PKC inhibitor Go6983-sensitive PKC subtype. Collectively, these results demonstrated that 18:1 LPE stimulates neurite outgrowth and protects against glutamate toxicity in cultured cortical neurons. These findings provide insights into the physiological or pathological roles of 18:1 LPE in the brain.

3-2 Introduction

Phospholipids are amphiphilic molecules composed of a hydrophilic head esterified by a hydrophobic fatty acid chain. They play crucial roles in various biological processes that range from structural integrity of cellular and organelle membranes to intracellular signal transduction [**20**]. Among the bioactive phospholipids, the roles of lysophospholipids in physiological and pathophysiological roles have attracted recent attention. Accumulating evidence suggests that lysophospholipids act as intercellular mediators. Lysophosphatidylethanolamine (LPE) is one of the lysophospholipids that can be generated from phosphatidylethanolamine (PE) via a phospholipase A-type reaction [**22**]. LPE is composed of a glycerol backbone with an ethanolamine head group, a phosphate group, and a single fatty acid chain. Like other lysophospholipids, multiple LPE species with different fatty acid lengths and degrees of saturation exist [**31**]. The functions of LPE have been reported in non-mammalian organisms such as bacteria, yeast, or plants [**53–55**]. The effects of LPEs vary among organisms. For example, palmitoleoyl-LPE (16:1 LPE) exhibits antifungal and antibacterial activity against gram-positive bacteria *Bacillus thuringiensis* and the yeast *Saccharomyces cerevisiae* [**54**], and an exogenous application of stearoyl-LPE (18:0 LPE) delays leaf senescence in plants [**55**]. It was previously reported that LPEs are a minor constituent of mammalian cell membranes [**31**]. Extracellularly, LPEs have been detected in human plasma and cerebrospinal fluid at submicromolar to micromolar concentrations [**56**–**59**].

However, the physiological significance of LPE with multiple species remains largely unknown in mammals. A few studies suggest the cell type-specific roles of LPE in mammalian cell cultures [**33–36**]. For example, the LPE extracted from *Grifola frondosa*, a kind of mushroom, stimulates neurite-like outgrowth of rat pheochromocytoma PC12 cells [**33**]. Oleoyl-LPE (18:1 LPE) stimulates chemotactic migration and cellular invasion in SK-OV3 human ovarian cancer cells [**34**]. In these cells and other cell lines, LPE activates several intracellular signaling cascades such as activation of mitogen-activated protein kinase (MAPK) or stimulation of intracellular Ca^{2+} concentration [**34**, **35**, **41–43**]. Of note, it is reported that the fatty acid length and degree of unsaturation are important for the cellular response of

LPE [**35**, **42**, **43**]. For example, in MDA-MB-231 human breast cancer cells, Ca2+ response is induced by 18:1 LPE and myristoyl-LPE (14:0 LPE), but not by palmitoyl-LPE (16:0 LPE) and 18:0 LPE [**35**]. To date, the specific receptors for LPEs have not been identified, but the actions of LPEs have been suggested to be mediated through G protein-coupled receptors (GPCRs) [**34**, **35**, **41–43**].

The brain is one of the most lipid-rich organs [**60**], and phospholipids play crucial roles in brain functions ranging from structural integrity of cellular and organelle membranes to neuronal signaling [**18**, **23**]. It has been reported that the brain contains multiple LPE species [**27**, **29**, **37**]. To date, the roles of some lysophospholipids, such as lysophosphatidic acid and sphingosine-1-phosphate, in the brain have been well studied [**23**, **61**]; however, the roles of LPEs remain largely unknown. Intriguingly, changes of LPE level in the brain have been reported in Alzheimer's model mice, postischemic cognitive impairment rat model, or traumatic brain injury [**27, 29, 37**]. These suggest the physiological or pathological significance of LPE in the brain functions.

In **chapter 2**, I reported that 16:0 LPE and 18:0 LPE stimulate neurite outgrowth in cultured cortical neurons. This previous study and other reports demonstrated that structurally different LPEs act as intercellular mediators that trigger distinct intracellular signaling cascades [**35, 42, 43**]. Thus, the characterization of LPE species composition in the brain and elucidation of their roles are essential for understanding the physiological and pathological significance of LPE in the brain. In this study, I performed quantitative liquid chromatography-electrospray ionization tandem mass spectrometry (LC-ESI-MS/MS) analysis of LPE species and showed their composition in the brain. I found that 18:1 LPE, which is one of the abundant LPE species in the brain, exerts the stimulation of neurite outgrowth and neuroprotective effect against glutamate toxicity in cultured cortical neurons. Furthermore, I demonstrate the potential signaling pathway involved in the actions of 18:1 LPE.

3-3 Result

3-3-1 Comprehensive LC-ESI-MS/MS analysis of LPE species in 4-week-old mice brain

To examine the species and amount of LPE in the brain, I performed the LC-ESI-MS/MS analysis using total lipids prepared from four-week-old C57BL/6N mice brain. The analysis revealed that docosahexaenoyl-LPE (22:6 LPE) was most abundant in the brain at approximately 4.2 nmol/mg weight of tissue, followed by docosatetraenoyl-LPE (22:4 LPE), 18:1 LPE, arachidonoyl-LPE (20:4 LPE) at approximately 1.5, 1.5, and 1.2 nmol/mg tissue weight, respectively **(Fig. 19)**. Other LPE species were detected at lower concentration.

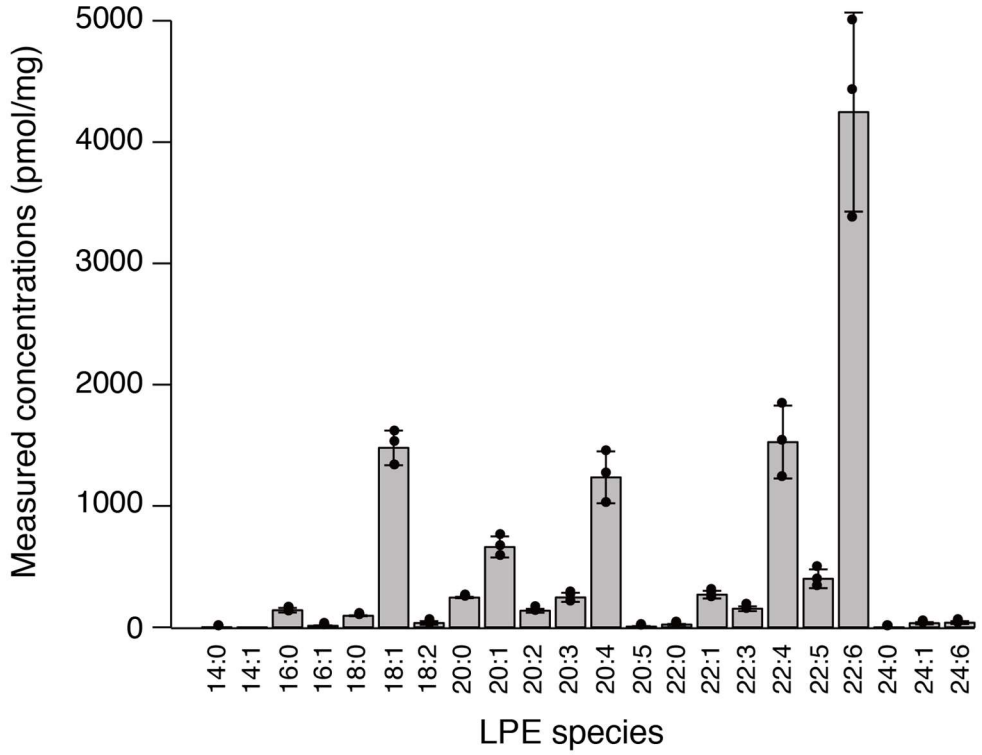

Fig. 19 Comprehensive LC-ESI-MS/MS analysis of LPE species in 4-week-old mice brain.

Comprehensive quantitative LC-ESI-MS/MS analysis of LPE species in four-week-old male mice brain. LPE molecular species were detected and quantified using LC-ESI-MS/MS. The amount of LPEs is represented by mol per mg tissue weight. All values represent mean ± SD. n = 3 mice.

3-3-2 Effects of 18:1 LPE on neurite outgrowth

In this study, I investigated the role of 18:1 LPE, because to the best of my knowledge, it was the only commercially available LPE among the abundant brain LPE species at the time of this study. The elucidation of 18:1 LPE roles in the central nervous system (CNS) neurons is important because 18:1 LPE is one of the abundant LPE species in the brain (**Fig. 19**). 18:1 LPE has been shown to be one of the LPE species increased in the hippocampus after global cerebral ischemia in rat [**27**]. Changed 18:1 LPE level in plasma has been suggested to be a potential biomarker for major depressive disorder patients [56] and Alzheimer's disease patients [**62**]. However, the roles of 18:1 LPE in CNS neurons remain unknown. To examine the effects of 18:1 LPE on neuronal morphology and viability, cultured cortical neurons were incubated with different concentrations of 18:1 LPE. I observed that 18:1 LPE dose-dependently increased the length of neurites at concentrations of 1–10 μM (**Fig. 20**). For neuronal cell viability, 5 μM or less of 18:1 LPE had little effect (**Fig. 20**). At concentrations of 10 μM or more, I observed a decrease in neuronal cell viability. Next, I examined the time course of 18:1 LPE effects on neurite outgrowth. The cultured cortical neurons were incubated with 1 μM 18:1 LPE and neurite outgrowth was analyzed. In the cultures incubated with 18:1 LPE, the lengths of the longest neurites were gradually increased from DIV1 to DIV3, which are significantly longer than those of control cultures (**Fig. 21**). The number of neurites emerging from the soma was also increased in the 18:1 LPE-treated cultures at DIV 2 compared with that in the control cultures. The number of branches for the longest neurite in the 18:1 LPE-treated cultures was comparable to those in the control cultures. Collectively, these results suggested that 18:1 LPE stimulates neurite outgrowth in cultured cortical neurons.

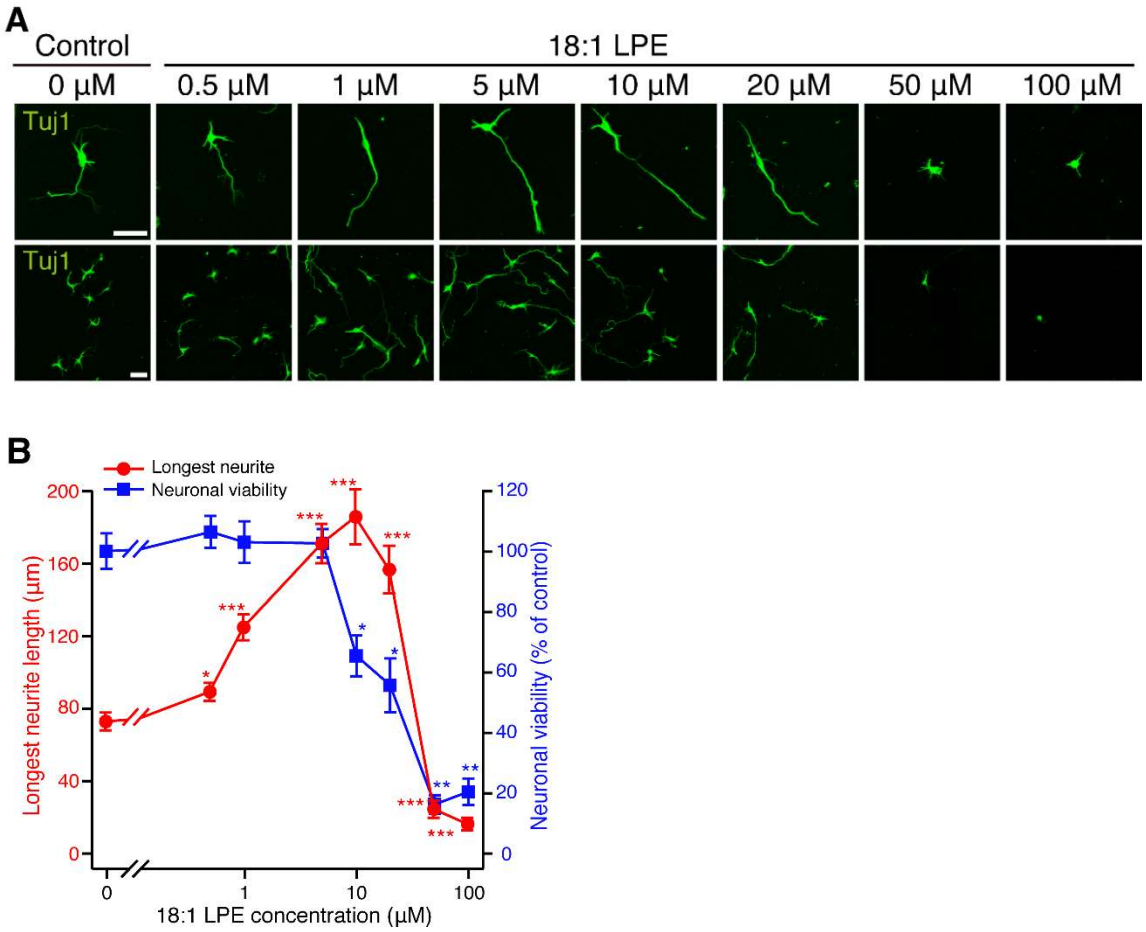

Fig. 20 Dose-dependent effects of 18:1 LPE on neurite outgrowth and neuronal cell viability. (**A)** Dose-dependent stimulation of neurite outgrowth by 18:1 LPE. The indicated 18:1 LPE concentrations were applied to the cultures at DIV0 and immunostained with anti-Tuj 1 antibody at DIV3 to visualize neurites of cortical neurons. (**B**) Quantification of the length of the longest neurite emerging from the soma and the neuronal cell viability in (A). Scale bar represents 50 µm. All values represent mean ± SEM. Statistical significance was evaluated using Kruskal–Wallis test followed by post hoc Steel–Dwass test: *** $p < 0.001$, ** $p < 0.01$, and * $p < 0.05$, n = 60 cells (neurite length) and n = 10 area (neuronal viability).

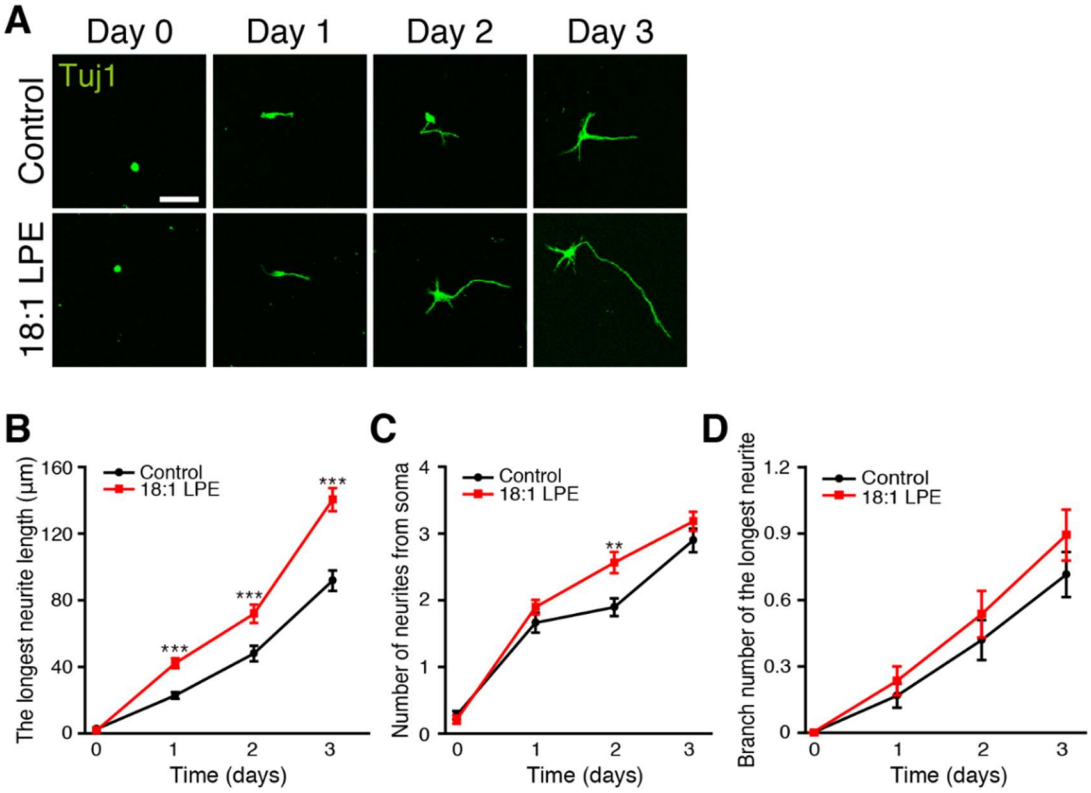

Fig. 21 Effects of 18:1 LPE on neurite outgrowth in cultured cortical neurons.

(**A**) Extracellular application of 18:1 LPE stimulates neurite outgrowth in cultured cortical neurons. (**B–D**) Quantification of the length of the longest neurite emerging from the soma (B), the number of neurites emerging from the soma (C), and the numbers of branches per longest neurite (D) in (A). The cultures were immunostained with anti-Tuji1 antibody to visualize neurites of cortical neurons in (A). Scale bar represents 50 μm. All values represent mean ± SEM. Statistical significance was evaluated using Mann–Whitney U test in (B)–(D): *** $p < 0.001$ and ** $p < 0.01$ vs. control, respectively, n = 60 cells.

3-3-3 Effects of inhibitors on 18:1 LPE-stimulated neurite outgrowth

Previous study has suggested that the actions of LPEs, 16:0 LPE and 18:0 LPE, are mediated by distinct GPCR-activated G protein-coupled PLC. To examine what type of G protein was involved in 18:1 LPE-stimulated neurite outgrowth, the cultured cortical neurons were incubated with Gq/11 inhibitor YM-254890 or Gi/Go inhibitor PTX. Application of YM-254890 inhibited 18:1 LPE-stimulated neurite outgrowth (**Fig. 22A, B**). In contrast, PTX had little effect on 18:1 LPE-stimulated neurite outgrowth (**Fig. 22C, D**). These results suggested that the action of 18:1 LPE is mediated by YM-254890-sensitive Gq/11 protein. It is known that Gq/11 activates phospholipase Cβ and initiates the Ca^{2+}/diacylglycerol-PKC-MAPK cascade [**63**]. To examine whether this signaling cascade is involved in 18:1 LPE-stimulated neurite outgrowth, PLC inhibitor U73122, PKC inhibitor Go6983, which inhibits PKCα, β, γ, δ, and ζ [**44**], or MAPK inhibitor U0126 was applied to the cultures. The application of U73122, Go6983, or U0126 inhibited 18:1 LPE-stimulated neurite outgrowth (**Fig. 23**). Combining these results with the G proteins inhibitor results suggested that Gq/11-PLC-PKC-MAPK signal cascade is involved in 18:1 LPE-stimulated neurite outgrowth in cultured cortical neurons.

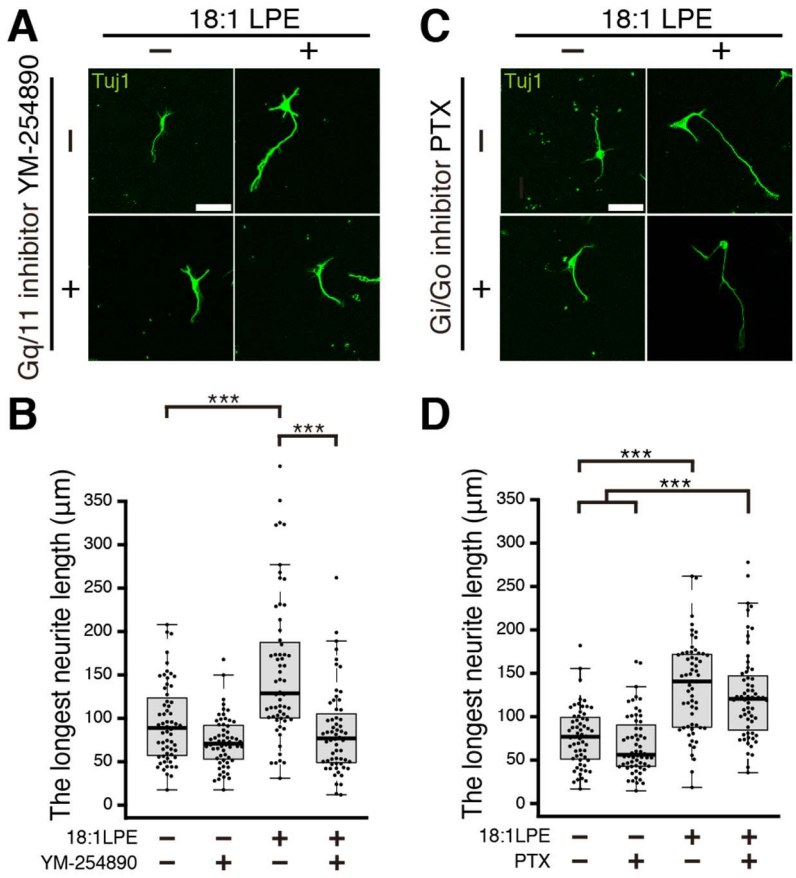

Fig. 22 Effects of G protein inhibitors on 18:1 LPE-stimulated neurite outgrowth in cultured cortical neurons. (**A**) Effects of Gq/11 inhibitor YM-254890 on 18:1 LPE-stimulated neurite outgrowth. Cultures were incubated with 1 μM 18:1 LPE in the presence or absence of 0.5 μM YM-254890. (**B**) Quantification of the length of the longest neurite in (A). (**C**) Effects of Gi/Go inhibitor PTX on 18:1 LPE-stimulated neurite outgrowth. Cultures were stimulated with 1 μM 18:1 LPE in the presence or absence of 1 ng/ml PTX. (**D**) Quantification of the length of the longest neurite in (C). 18:1 LPE and inhibitors were applied to the cultures at DIV0 and fixed at DIV3. This was followed by immunostaining with anti-Tuj 1 antibody to visualize neurites of cortical neurons in (A) and (C). Scale bars represent 50 μm. The horizontal line in each box indicates the median, the box shows the IQR, and the whiskers are 1.5× IQR. Statistical significance was evaluated using the Kruskal–Wallis test followed by post hoc Steel–Dwass test. *** $p < 0.001$, n = 60 cells.

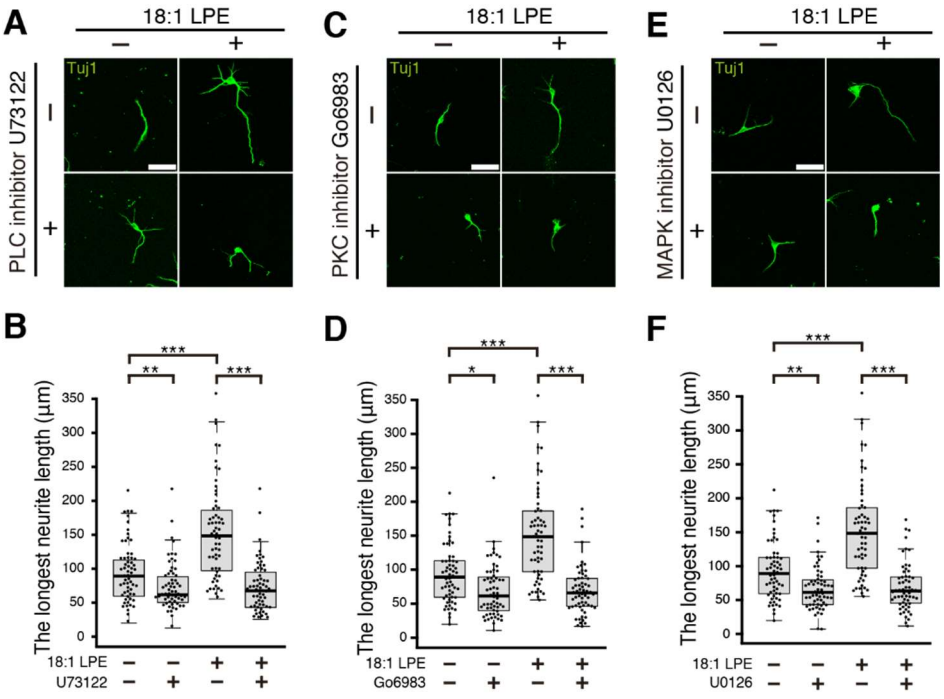

Fig. 23 Effects of PLC, PKC, and MAPK inhibitors on 18:1 LPE-stimulated neurite outgrowth in cultured cortical neurons.

(**A**) Effects of PLC inhibitor U73122 on 18:1 LPE-stimulated neurite outgrowth. Cultures were stimulated with 1 μM 18:1 LPE in the presence or absence of 0.5 μM U73122. (**B**) Quantification of the length of the longest neurite in (A). (**C**) Effects of PKC inhibitor Go6983 on 18:1 LPE-stimulated neurite outgrowth. Cultures were stimulated with 1 μM 18:1 LPE in the presence or absence of 1 μM Go6983. (**D**) Quantification of the length of the longest neurite in (C). (**E**) Effects of MAPK inhibitor U0126 on 18:1 LPE-stimulated neurite outgrowth. Cultures were stimulated with 1 μM 18:1 LPE in the presence or absence of 5 μM U0126. (**F**) Quantification of the length of the longest neurite in (E). 18:1 LPE and inhibitors were applied to the cultures at DIV0 and fixed at DIV3. This was followed by immunostaining with anti-Tuj 1 antibody to visualize neurites of cortical neuron in (A), (C), and (E). The horizontal line in each box indicates the median, the box shows the IQR, and the whiskers are 1.5× IQR. Statistical significance was evaluated using the Kruskal–Wallis test followed by post hoc Steel–Dwass test. *** $p < 0.001$, ** $p < 0.01$, and * $p < 0.05$, n = 60 cells.

3-3-4 18:1 LPE activate MAPK in cultured cortical neurons

Next, examined whether Gq/11-PLC-PKC-MAPK signal cascade was activated in 18:1 LPE-treated cultured cortical neurons. The cultured cortical neurons were incubated with 18:1 LPE and subjected to Western blot analysis using anti-phospho-ERK1/2 and anti-ERK1/2 antibodies. Anti-ERK1/2 antibody detected the bands corresponding to the size of ERK1/2 in all conditions (**Fig. 24A**). The application of 18:1 LPE significantly increased phosphorylated ERK1/2 signals in a dose-dependent manner at a concentration of 1–50 μM; however, no further increase was detected at a concentration of 100 μM (**Fig. 24A and B**). When the cultures were treated with MAPK inhibitor U0126 at 5 μM, phosphorylated ERK1/2 signals were not detected in control and 18:1 LPE-applied cultures (**Fig. 24C and D**). These results suggest that 18:1 LPE activates MAPK/ERK1/2 in cultured cortical neurons.

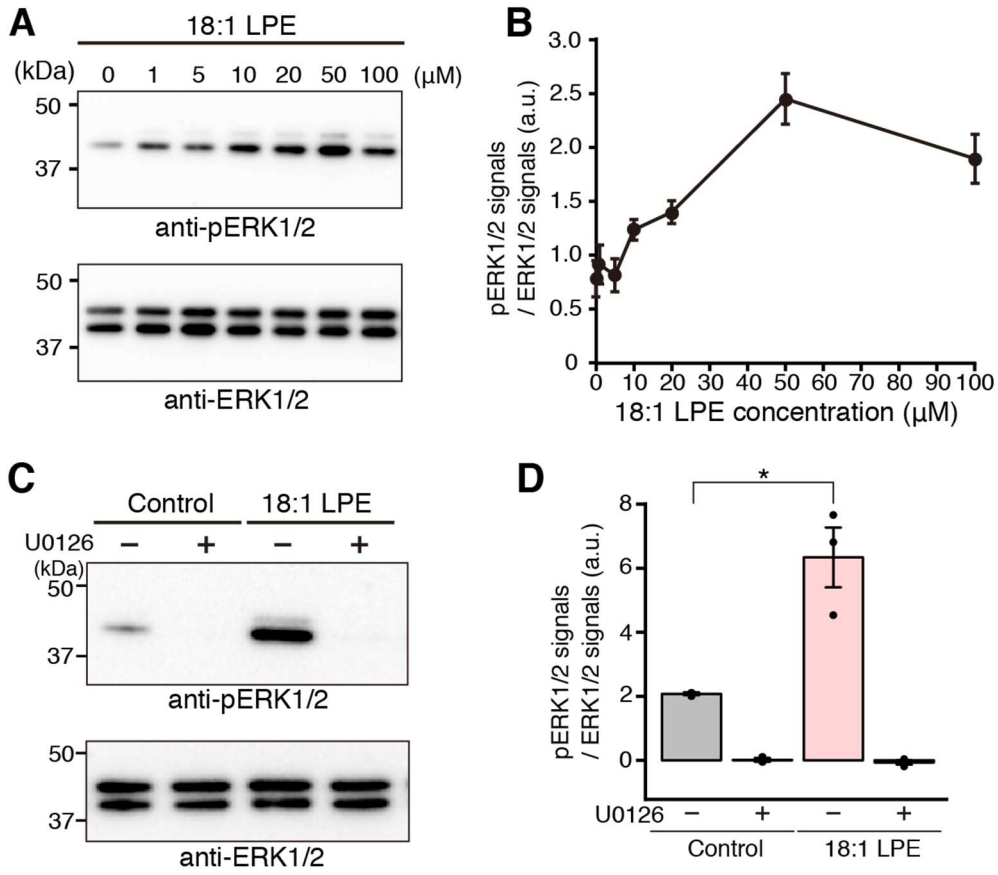

Fig. 24 18:1 LPE activates MAPK in cultured cortical neurons.

(**A**) Activation of MAPK in 18:1 LPE-treated cultures. Indicated 18:1 LPE concentrations were applied to the cultures at DIV7 and incubated for 10 min. Cell lysates were separated by SDS-PAGE and immunoblotted with anti-pERK1/2 and anti-ERK1/2 antibodies. (**B**) Quantification of phosphorylated ERK1/2 signals in (A). The intensities of phosphorylated ERK1/2 signals were normalized with those of ERK1/2 signals. (**C**) MAPK inhibitor U0126 inhibits 18:1 LPE-induced phosphorylation of ERK1/2. Cultures were incubated with 50 μM 18:1 LPE, with or without 5 μM MAPK inhibitor U0126. Cell lysates were separated using SDS-PAGE and immunoblotted with anti-pERK1/2 and anti-ERK1/2 antibodies. (**D**) Quantification of phosphorylated ERK1/2 signals in (C). Phosphorylated ERK1/2 signal intensities were normalized with those of ERK1/2 signals. All values represent mean ± SEM. Statistical significance was evaluated using one-way ANOVA followed by *post hoc* Tukey's test. * $p < 0.05$, n = 6 cultures in (B), and n = 3 cultures in (D).

3-3-5 Protective effect of 18:1 LPE on glutamate-induced neurotoxicity

Recent reports showed that 18:1 LPE is increased in the hippocampus after brain ischemia in rat [**27**, **64**]. These previous observations raise the intriguing possibility that 18:1 LPE is involved in the protection against glutamate excitotoxicity. To examine this, the cultured cortical neurons were exposed with glutamate with or without 18:1 LPE (**Fig. 25**). When the cultures were exposed with 3 μM glutamate at DIV14 for 48 h, the number of calcein and NeuN double-positive living neurons was dramatically decreased (**Fig. 26**). The application of 10 μM 18:1 LPE significantly increased the number of living neurons compared to that in cultures only treated with glutamate. These results suggested that 18:1 LPE protects cortical neurons from glutamate-induced cell death.

Additionally, a minor LPE species in mouse brain, 16:0 LPE and 18:0 LPE also showed the same effect on glutamate-induced neurotoxicity (**Fig. 27**).

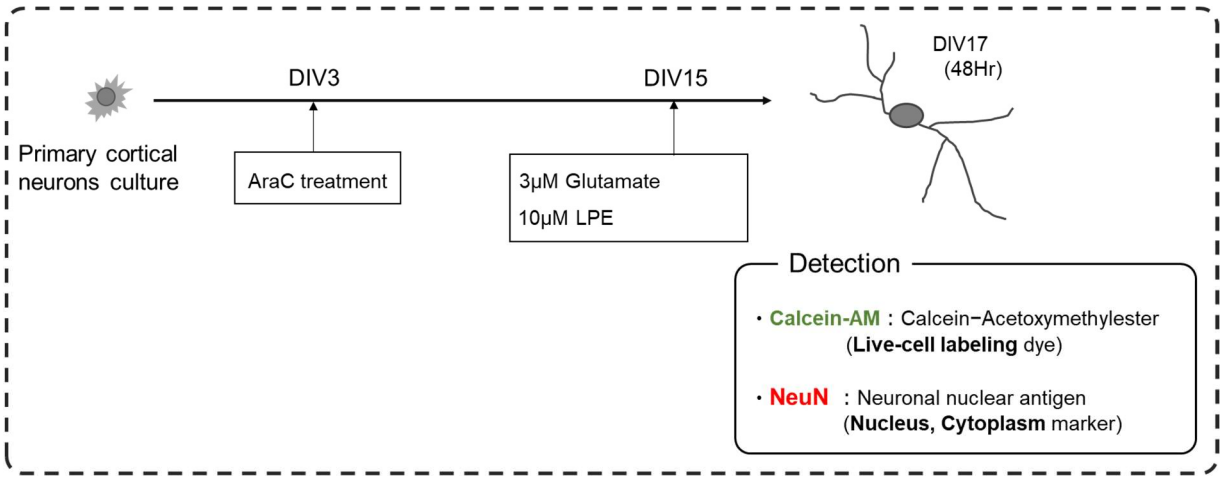

Fig. 25 Schematic overview of the experiment on effects of LPEs on glutamate-induced neurotoxicity.

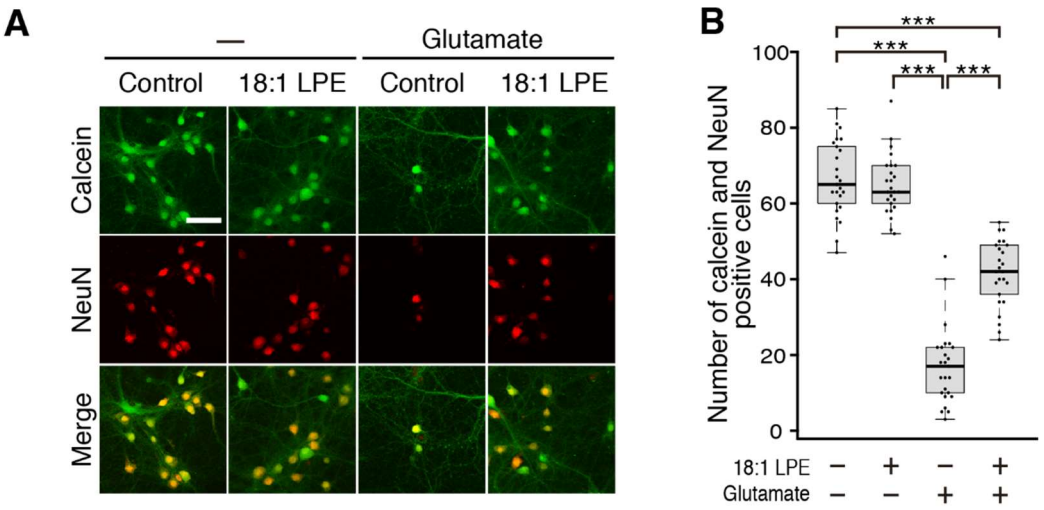

Fig. 26　18:1 LPE protects cultured cortical neurons from glutamate toxicity.

(**A**) Effects of 18:1 LPE on glutamate-induced neurotoxicity. Cells were incubated with 3 μM glutamate, with or without 10 μM 18:1 LPE, and stained with calcein and anti-NeuN antibody.

(**B**) Quantification of number of calcein and NeuN double-positive cells in (A). Scale bar represents 50 μm. The horizontal line in each box indicates the median, the box shows the IQR, and the whiskers are 1.5× IQR. Statistical significance was evaluated using the Kruskal–Wallis test followed by post hoc Steel–Dwass test. *** $p < 0.001$, n = 25 areas.

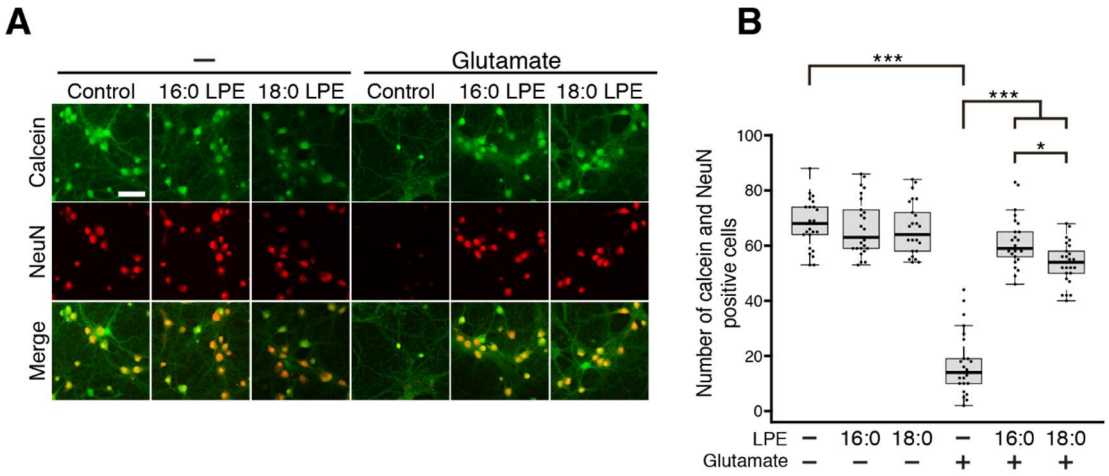

Fig. 27 16:0 LPE and 18:0 LPE protect cultured cortical neurons from glutamate-induced neurotoxicity. (**A**) Effects of 16:0 LPE and 18:0 LPE on glutamate-induced neurotoxicity. (**B**) Quantification of number of calcein and NeuN double-positive cells in (A). Scale bar represents 50 μm. The horizontal line in each box indicates the median, the box shows the IQR, and the whiskers are 1.5× IQR. Statistical significance was evaluated with the Kruskal–Wallis test followed by post hoc Steel–Dwass test. *** $p < 0.001$ and * $p < 0.05$, n = 25 areas.

Finally, I examined the signal cascades involved in 18:1 LPE-mediated protection of glutamate toxicity with inhibitors used in neurite outgrowth experiments. When Gq/11 inhibitor YM-254890, Gi/Go inhibitor PTX, PLC inhibitor U73122, or MAPK inhibitor U0126 was applied to the cultured cortical neurons, these inhibitors exerted protective effects on glutamate toxicity even in the absence of 18:1 LPE (**Fig. 28**), presumably due to inhibition of the signal cascade involved in the glutamate-induced neurotoxicity [**65–67**]. Therefore, I could not examine the involvement of these signaling cascades. On the other hand, PKC inhibitor Go6983 had little effect on glutamate toxicity (**Fig. 29**). Thus, I examined the involvement of Go6983-sensitive PKC subtype in 18:1 LPE-mediated protection of glutamate toxicity. Application of Go6983 completely inhibited the protective effect of 18:1 LPE on glutamate toxicity (**Fig. 29**). These results suggested that, at least, Go6983-sensitive PKCα, β, γ, δ, and/or ζ are involved in 18:1 LPE-mediated protection from glutamate toxicity.

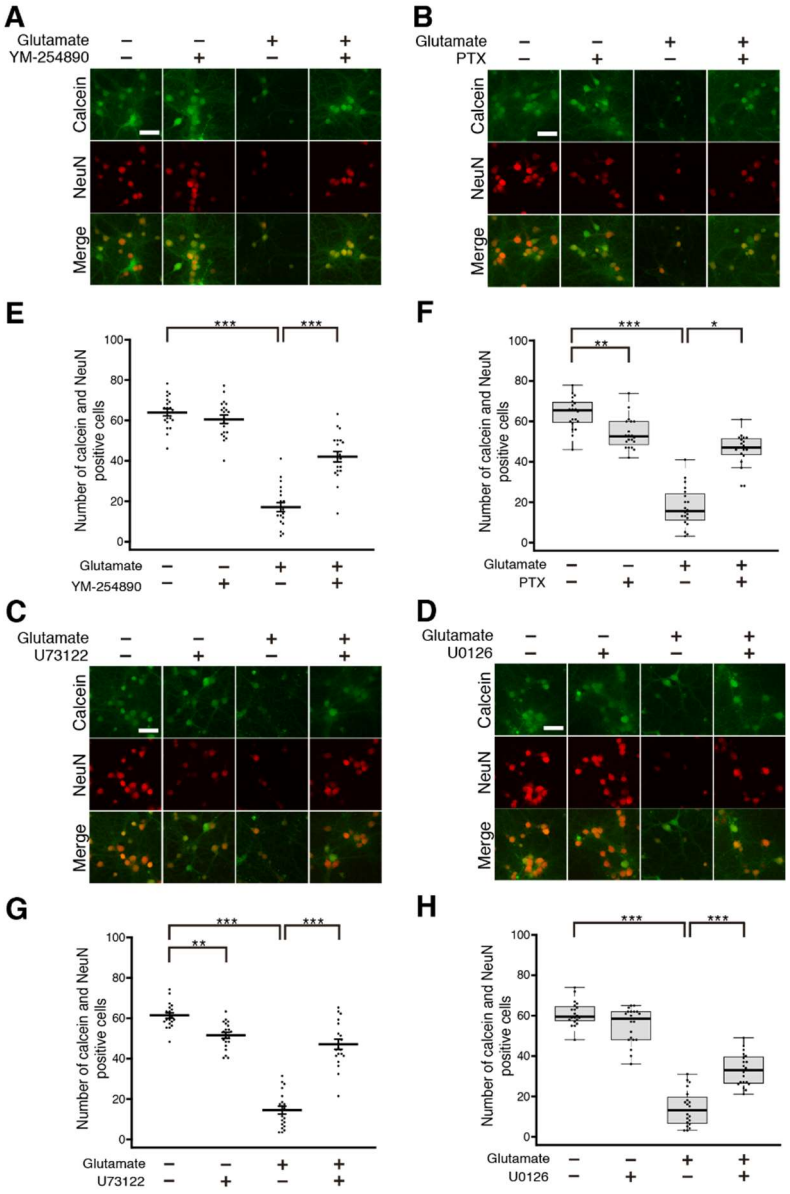

Fig. 28 Effects of inhibitors of signaling molecules on glutamate-induced neurotoxicity.

(**A**–**D**) Effects of Gq/11 inhibitor YM-254890 (A), Gi/Go inhibitor PTX (B), PLC inhibitor U73122 (C), and MAPK inhibitor U0126 (D) on glutamate-induced neurotoxicity. Indicated combination of 10 μM 18:1 LPE, 3 μM glutamate, and inhibitors were applied to the cultures. (**E**–**H**) Quantification of the number of calcein and NeuN double-positive cells in (A), (B), (C), and (D). Scale bars represent 50 μm. All values represent mean ± SEM in (E) and (G). The horizontal line in each box indicates the median, the box shows the IQR, and the whiskers are 1.5× IQR in (F) and (H). Statistical significance was evaluated with one-way ANOVA followed by Tukey's *post hoc* test in (E) and (G), or the Kruskal–Wallis test followed by post hoc Steel–Dwass test in (F) and (H). *** $p < 0.001$, ** $p < 0.01$, and * $p < 0.05$, n = 20 areas from 2–3 cultures.

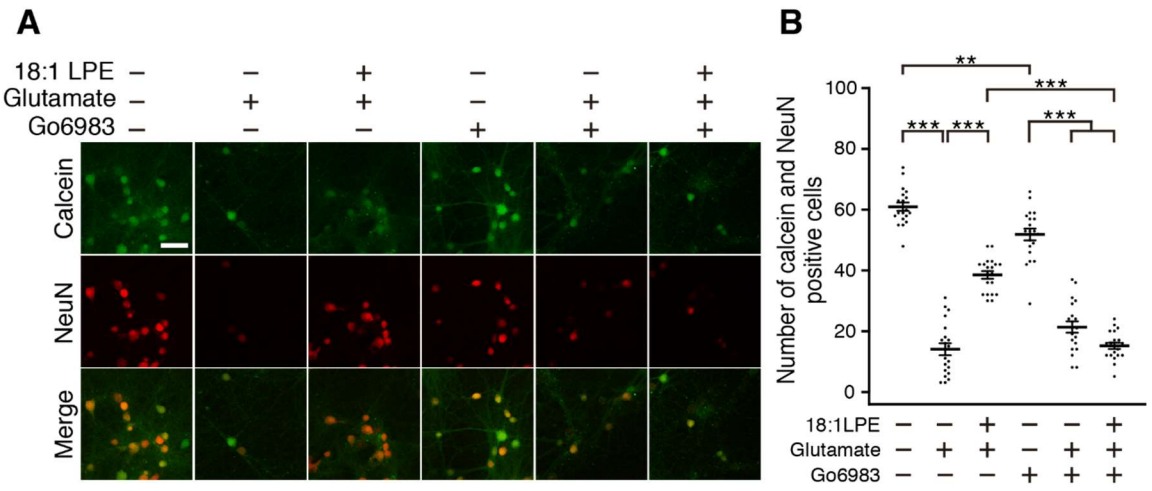

Fig. 29 18:1 LPE-mediated protective effects are inhibited by PKC inhibitor Go6983.

(A) Effects of PKC inhibitor Go6983 on 18:1 LPE-mediated protection of glutamate toxicity. Indicated combination of 10 μM 18:1 LPE, 3 μM glutamate, and 1 μM Go6983 were applied to the cultures. The cultures were stained with calcein and anti-NeuN antibody. **(B)** Quantification of number of calcein and NeuN double-positive cells in (A). Scale bar represents 50 μm. All values represent mean ± SEM in. Statistical significance was evaluated using one-way ANOVA followed by *post hoc* Tukey's test. ** $p < 0.01$, *** $p < 0.001$, n = 20 areas.

3-4 Discussion

Lysophospholipids are bioactive molecules that exert pleiotropic effects on various type cells [**22**]. In this study, I performed comprehensive LC-ESI-MS/MS analysis of LPE species and showed composition in mouse brain. This study demonstrates that 18:1 LPE, which is one of the abundant LPE species in the brain, exerts the stimulation of neurite outgrowth and neuroprotective effects against glutamate-induced excitotoxicity in cultured cortical neurons.

It is known that many structurally different LPE species with different fatty acid lengths and degrees of saturation exist in mammals [**31**]. Consistent with this observation, LC-ESI-MS/MS analysis detected 22 LPE species in four-week-old male mice brain, but their amounts vary from nano mol to low pico mol per mg tissue weight (**Fig. 19**). Quantitative analysis showed that 18:1, 20:4, 22:4, and 22:6 LPE are abundant LPE species in the brain. In contrast, 16:0 LPE and 18:0 LPE, which I previously reported as neurite outgrowth-stimulating molecules (**Chapter 2**), are less abundant (**Fig. 19**). The composition of LPE species differs among organs. For example, 16:0 LPE and 18:0 LPE, which are less abundant in mouse brain, are most abundant LPE species in rat liver [**68**]. These may imply the functional differences among LPE species in different organs. However, the physiological roles of LPE with multiple species remain largely unknown in mammals. A few studies suggest the cell type-specific roles of LPE species in mammalian cell cultures [**33–36**].

My results show that 18:1 LPE, one of abundant LPE species in brain, stimulates neurite outgrowth in cultured cortical neurons (**Fig. 20 and 21**). Noteworthy, the effect of 18:1 LPE on neurite outgrowth was inhibited by Gq/11 inhibitor YM-254890 but not by Gi/Go inhibitor PTX (**Fig. 22**). Interestingly, in contrast to 18:1 LPE that has mono-unsaturated fatty acid chain, my recent study showed that the saturated 18:0 LPE-stimulated neurite outgrowth is inhibited by PTX but not by YM-254890 (**Chapter 2**). Thus, the degree of saturation of fatty acid chain in LPE would be important for receptor recognition. Consistent with my observation, a few studies suggest that distinct GPCRs mediate the actions of different LPE species [**42**, **43**]. In terms of signal cascade, 18:1 LPE-stimulated neurite outgrowth was inhibited by PLC

inhibitor U73122, PKC inhibitor Go6983, or MAPK inhibitor U0126 (**Fig. 23**). Furthermore, 18:1 LPE activated MAPK/ERK1/2 (**Fig. 24**). These results collectively suggest that PLC-PKC-MAPK pathway is involved in 18:1 LPE action. Involvement of PLC-PKC-MAPK signaling pathway is also suggested in the action of 18:0 LPE on neurite outgrowth (**Chapter 2**). Interestingly, in terms of PKC, 16:0 LPE-stimulated neurite outgrowth, which is sensitive to YM-254890, is not inhibited by PKC inhibitor Go6983 (**Chapter 2**). It is known that LPE is converted to other phospholipids, i.e., LPE is converted to LPA by autotaxin extracellularly and LPE is converted to PE intracellularly [**69**, **70**]. However, neither LPA nor PE stimulates neurite outgrowth in cultured cortical neurons (**Fig. 30**).

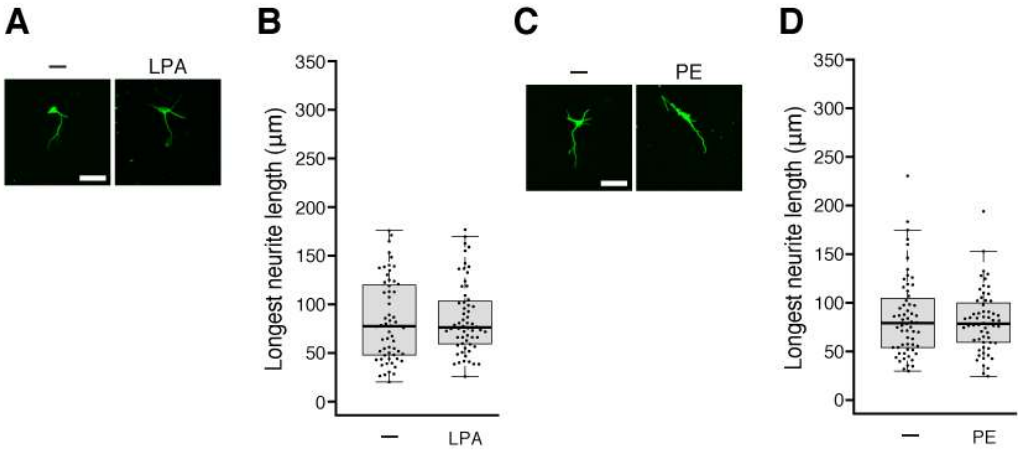

Fig. 30 Effects of LPA and PE on neurite outgrowth.

(A) Effects of LPA on neurite outgrowth. The cultured cortical neurons were incubated with 1 μM 18:1 LPA. **(B)** Quantification of the length of the longest neurite emerging from the soma. **(C)** Effects of PE on neurite outgrowth. The cultured cortical neurons were incubated with 1 μM natural PE. **(D)** Quantification of the length of the longest neurite emerging from the soma. 18:1 LPA and natural PE were applied to the cultures at DIV0 and fixed at DIV3. This was followed by immunostaining with anti-Tuj1 antibody to visualize neurites of cortical neuron in (A) and (C). Scale bars represent 50 μm in (A) and (C). The horizontal line in each box indicates the median, the box shows the IQR, and the whiskers are 1.5× IQR. Statistical significance was evaluated using Mann–Whitney U test. n = 60 cells.

In the cultured cortical neurons, the application of 18:1 LPE protects neurons from glutamate-induced excitotoxicity (**Fig. 26**). In cultured cortical neurons, I observed that the glutamate-induced excitotoxicity was suppressed by the Gq/11 inhibitor YM-254890, PLC inhibitor U73122, and MAPK inhibitor U0126, suggesting that the Gq/11-PLC-PKC-MAPK signal pathway activation is required for glutamate stimulated signals for excitotoxicity. This may appear contradictory to my data suggesting 18:1 LPE protects neurons against glutamate excitotoxicity and activates the Gq/11-PLC-PKC-MAPK pathway in the context of neurite outgrowth. MAPK/ERK1/2 is reportedly involved in both cell death and survival [**71**, **72**]. Thus far, how MAPK/ERK1/2 promotes neuronal cell death or neuronal survival is not completely clarified. However, it is suggested that the duration of ERK1/2 activation is one of the factors that determine cell outcomes, i.e., a sustained and prolonged ERK1/2 activation observed after 6 h of glutamate treatment generates a pro-death signal [**71**]. In contrast, the transient activation of ERK1/2 by brain-derived neurotrophic factor provides a protective signal against glutamate toxicity [**71**]. In my cultured cortical neurons, I found that 18:1 LPE transiently activates ERK1/2 (**Fig. 31**). Therefore, the same signal pathway could be activated under both glutamate and 18:1 LPE stimulations, but transient ERK1/2 activation may be important for the neuroprotective effects of 18:1 LPE.

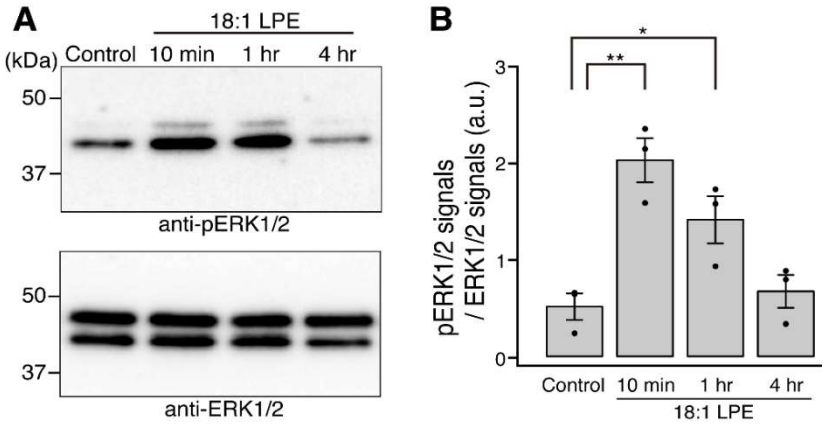

Fig. 31 Transient activation of ERK1/2 by 18:1 LPE.

(A) The time course of phosphorylation of ERK1/2 in the cultured cortical neurons. Cultures were incubated with 50 μM 18:1 LPE for 10 min, 1 hr, or 4 hr. The cell lysates were separated by SDS-PAGE and immunoblotted with anti-pERK1/2 and anti-ERK1/2 antibodies. **(B)** Quantification of phosphorylated ERK1/2 signals in (A). The intensities of phosphorylated ERK1/2 signals were normalized with those of ERK1/2 signals. All values represent mean ± SEM. Statistical significance was evaluated using one-way ANOVA followed by post hoc Dunnett's test. ** $p < 0.05$ and * $p < 0.05$, n = 3 cultures.

I showed that the PKC inhibitor Go6983 suppressed the protective effects of 18:1 LPE, suggesting that the activation of Go6983-sensitive PKCα, β, γ, δ, and/or ζ is required for the protective effects of 18:1 LPE (**Fig. 29**). PKC activation is reported to exert protective effects on glutamate toxicity [**73**]. In contrast, Go6983 had little effect on glutamate induced neuronal cell death (**Fig. 29**). Combined with the results of protective effects of Gq/11, PLC, and MAPK inhibitors (**Fig. 28**), these data suggest that the Go6983-insensitive PKC is involved in glutamate-induced neuronal cell death.

Thus, different types of PKC could be activated in glutamate-induced neuronal death and 18:1 LPE-mediated protection processes. Intriguingly, it has reported that 18:1 LPE is upregulated in the hippocampus after global cerebral ischemia [**27**, **64**]. Additionally, changes of 18:1 LPE level in brain have been reported in pathophysiological conditions such as Alzheimer's model mice [**37**]. These

previous studies imply two possible functions of 18:1 LPE. First, 18:1 LPE protects brain from pathophysiological condition. Second, LPE is involved in the development of pathophysiological conditions. My results of the neuroprotective effect of 18:1 LPE against glutamate-induced excitotoxicity (**Fig. 26**) prefer the former possibility, since neuronal cell death by excitotoxicity is thought to be one of the common mechanisms of neuronal cell death among cerebral ischemia, brain trauma, and Alzheimer disease [**74**]. In Alzheimer's model mice [**37**], traumatic brain injury rat model [**29**], and global cerebral ischemia rat [**27**, **64**], 22:6 LPE is also upregulated in the hippocampus, but the roles of 22:6 LPE remain unknown.

In conclusion, I found that 18:1 LPE stimulates neurite outgrowth and protects against glutamate toxicity in cultured cortical neurons. These findings establish a basis for further investigations into the role of LPEs in the brain. Thus far, the functions of other abundant LPE species, i.e., 20:4 LPE, 22:4 LPE, and 22:6 LPE, remain unknown. Therefore, it is important to purify these LPEs from brain tissue or initiate their biochemical synthesis to analyze and characterize their roles. Moreover, the identification of receptors for each LPE and elucidation of their signaling will be key to understanding the physiological and pathological roles of LPE in the brain.

3-5 Material and Methods

3-5-1 Mass spectrometric analyses of Phospholipids

For analysis of LPE species in the brain, 4-week-old mice that had completed neural network formation were used. Under deep anesthesia, four-week-old C57BL/6N male mice were perfused transcardially with ice cold phosphate-buffered saline for 2 min. Whole brains were dissected and stored in liquid N_2 until sample preparation. Comprehensive lipid analysis was described previously [**75**, **76**]. Briefly, total lipids were extracted from the samples according to the Bligh-Dyer method [**77**]. An aliquot of the lower/organic phase was evaporated to dryness under N_2 and the residue was dissolved in methanol for LC-ESI-/MS/MS measurements of LPE. LC-ESI-MS/MS analysis was performed using an UltiMate 3000 LC system (Thermo Fisher Scientific) equipped with HTC PAL autosampler (CTC Analytics). The lipids were separated on Waters XBridge C18 column (3.5 μm, 150 mm × 1.0 mm i.d.) at room temperature (25°C) using a gradient solvent system as follows: mobile phase A (isopropanol/methanol/water (5/1/4 v/v/v) supplemented with 5 mM of ammonium formate and 0.05% ammonium hydroxide solution)/mobile phase B (isopropanol supplemented with 5 mM ammonium formate and 0.05% ammonium hydroxide solution) ratios of 60%/40% (0 min), 40%/60% (0–1 min), 20%/80% (1–9 min), 5%/95% (9–11 min), 5%/95% (11–30 min), 95%/5% (30–31 min), 95%/5% (31–35 min), and 60%/40% (35–45 min). The flow rate was 25 μl/min. The lipid species were measured by the selected reaction monitoring in the positive ion mode with a triple-stage quadrupole mass spectrometer (TSQ Vantage AM, Thermo Fisher Scientific). The characteristic fragments of individual lipids were detected by the product ion scan (MS/MS mode). 17:1 LPE was used for internal standard calibration.

3-5-2 Cell cultures

Primary cortical neuron cultures were prepared from ICR mice and maintained as described previously (**Chapter 2**). In brief, the primary cortical neurons prepared from ICR mice at embryonic day 18 were cultured in Neurobasal-A supplemented with 2% B-27 supplement (Thermo Fisher Scientific), 5% fetal calf serum (FCS), 100 U/ml penicillin, 100 μg/ml streptomycin, and 0.2 mM GlutaMax-I (Thermo Fisher Scientific) for 5 h and then cultured in the same medium without FCS. All cell culture assays were performed under FCS-free conditions. For morphological analysis, the cells were placed on 12-diameter coverslips coated with 30 μg/ml poly-L-lysine (weight 70–150 kDa; Sigma-Aldrich) and 10 μg/ml mouse laminin (Thermo Fisher Scientific) at a density of 1.0×10^5 cells/well on 24-well culture plates. For Western blot analysis and glutamate toxicity assay, the cells were plated on a 24-well dish at a density of 5.0×10^5 cells/well. For glutamate toxicity assay, 4 μM 1-β-D-arabino-furanosyl-cytosine (AraC) was applied to the culture medium at 3 days in vitro (DIV3) and the medium was changed at DIV7 by replacing half of the old medium with a fresh one. All animal procedures were approved by the Animal Care and the Use Committee of Shinshu University (Approval No. 290072 and 020078).

3-5-3 Morphological analysis

Morphological analysis was performed essentially as described previously (**Chapter 2**). For analyzing the effects of phospholipids on neurite outgrowth, 1 μM 18:1 LPE (1-Oleoyl-LPE; Avanti), 1 μM lysophosphatidic acid (LPA) (1-oleoyl-LPA sodium salt; Tocris Bioscience), or 1 μM phosphatidylethanolamine (PE) (Avanti) was applied to the culture medium at DIV0. For inhibitor experiments, the cultures were treated with inhibitors in the presence or absence of 1 μM 18:1 LPE at DIV0. The cultures were fixed with 4% paraformaldehyde/4% sucrose at DIV3, except for analysis of the time course of neurite outgrowth. The fixed cells were incubated with PBS buffer containing 0.25%

Triton X-100 for 5 min. After blocking with 10% donkey serum, the cells were immunostained with mouse anti-Tuj1 antibody (neuron-specific class III β-tubulin, 1:5000; BioLegend), followed by incubation with donkey Alexa Fluor 488-conjugated anti-mouse IgG antibody (1:500; Thermo Fisher Scientific). The inhibitors used were as followed: Gi/Go inhibitor pertussis toxin (PTX) (1 ng/ml; Wako Pure Chemical Industries), Gq/11 inhibitor YM-254890 (0.5 μM; Wako Pure Chemical industries), phospholipase C (PLC) inhibitor U73122 (0.5 μM; Cayman Chemical), MAPK inhibitor U0126 (5 μM; Cayman Chemical), and protein kinase C (PKC) inhibitor Go6983 (1 μM; Cayman Chemical).

3-5-4 Western blot analysis

Primary cortical neuron cultures were prepared as described above and plated on the 24-well dish at a density of 5.0×10^5 cells /well. One to 100 μM 18:1 LPE or 18:0 LPE was applied to the culture medium at DIV7. For inhibitor experiment, the cultures were incubated with 100 μM 18:1 LPE or 18:0 LPE, with or without 5 μM U0126. After 10 min incubation, the cultures were solubilized with SDS sample buffer containing 2% SDS, 50 mM-Tris-HCI, pH6.8, 10% glycerol, 100 mM dithiothreitol, phosphatase inhibitor cocktail (Nakarai Tesque), and 0.025% Bromophenol Blue, followed by boiling at 95℃ for 10 min. For inhibition of MAPK, 5 μM MAPK inhibitor U0126 was applied to the cell culture medium 30 min before treatment with LPEs. The cell lysates were separated by SDS-polyacrylamide gel electrophoresis and transferred to PVDF membrane. After blocking with PVDF Blocking Reagent for Can Get Signal (TOYOBO), the membranes were incubated with mouse anti-phospho-MAPK/ERK1/2 (Thr202/Tyr204) antibody(E10, 1:2000; Cell Signaling Technology), followed by incubation with horseradish-peroxidase-conjugated secondary antibody. After stripping, the membranes were probed with rabbit anti p44/42 MAPK (ERK 1/2) antibody (1:1000; Cell Signaling Technology), followed by incubation with horseradish-peroxidase-conjugated secondary antibody. Can Get Signal Immunoreaction

Enhancer Solution (TOYOBO) was used for dilution of antibodies. The proteins were visualized by ECL Select Western Blotting Detection System (GE Healthcare) and detected by Las-4000 mini luminescent imaging analyzer (GE Healthcare). The quantification analysis was performed using ImageQuant TL image analysis software (GE Healthcare). Intensities of phosphorylated ERK1/2 signals were normalized with those of ERK1/2 signals.

3-5-5 Glutamate toxicity assay

At DIV14, the cortical cultured neurons were incubated with 10 μM 18:1 LPE or 18:0 LPE for 1 hr, and then incubated with 3 μM glutamate. After 48 hr, the living cells were staining Calcein-AM (Dojin Chemical) according to the manufacture's instruction, followed by fixed with 4%FPA. The fixed cells were incubated with anti-NeuN (1:500; Merk Millipore), followed by incubation with donkey Alexa Fluor 555-conjugated anti-mouse IgG antibody (1:500; Thermo Fisher Scientific). For inhibitor experiment, inhibitors were applied to the culture medium 30 min before LPE treatment. The concentrations of Inhibitors are the same as in morphological analysis.

3-5-6 Image acquisition and quantification

Images of culture experiments were taken with a confocal laser-scanning microscope (TCS SP8; Leica Microsystems) using HC PL APO CS2 20×/0.75 NA multiple immersion lens (Leica Microsystems) or HC PL APO CS 10×/0.40 NA multiple immersion lens (Leica Microsystems) under constant conditions. For analysis of the time course of neurite outgrowth, z-series of optical sections were projected by the brightest point method. Neurite of cortical neurons was identified by Tuj1 signals, and the length of the longest neurite, the number of neurites emerging from the soma, and the numbers of branches per longest

neurite were measured. All quantitative measurements were performed with ImageJ 1.52a software.

3-5-7 Statistical analysis

The results of at least two independent experiments were subjected to statistical analyses. Statistical significance was evaluated using one-way ANOVA followed by Tukey's test, Dunnett's *post hoc* test, or Student's t-test for parametric data analysis. Mann–Whitney U test or Kruskal–Wallis test followed by post hoc Steel–Dwass or Steel's test was used for non-parametric data analysis. All statistical analyses were performed using the R software (R Core Team, 2017). Statistical significance was assumed when $p < 0.05$.

4 Conclusion

This thesis is the first report to elucidate the role of LPEs in CNS neurons.

In **chapter 2**, I reported that the structurally different LPE species, 16:0 LPE and 18:0 LPE stimulate neurite outgrowth through distinct signaling cascades in cultured cortical neurons and that distinct G protein-coupled receptors are involved in these processes.

In **chapter 3**, I reported that 18:1 LPE, one of the abundant LPE species in brain, functions in protection of glutamate-induced excitotoxicity and stimulation of neurite outgrowth in cultured cortical neurons.

Combined with these results, it is suggesting that LPE function to protect of glutamate-induced excitotoxicity and stimulate neurite outgrowth in cultured cortical neurons.

Additionally, my results suggest that different types of GPCRs are likely to involve in the LPE-induced neurite outgrowth or glutamate toxicity depending on the difference in fatty acid length or degree of unsaturation.

This establishes the grounds for further investigation of the role of LPEs in the brain, including in recovery from trauma and in pathophysiology.

5 Bibliography

[1] Horner PJ, Gage FH. Regenerating the damaged central nervous system. *Nature*, **407**, 963–970 (2000).

[2] Kiryushko D, Berezin V, Bock E. Regulators of neurite outgrowth: role of cell adhesion molecules. *Ann N Y Acad Sci.*, **1014**, 140–154 (2004).

[3] Kulkarni VA, Firestein BL. The dendritic tree and brain disorders. *Mol Cell Neurosci.*, **50**, 10–20 (2012).

[4] Stoeckli ET. Understanding axon guidance: are we nearly there yet? *Development*, **145**, dev151415 (2018).

[5] Lotto B, Upton L, Price DJ, Gaspar P. Serotonin receptor activation enhances neurite outgrowth of thalamic neurons in rodents. *Neurosci Lett.*, **269**, 87–90 (1999).

[6] Cibelli G, Corsi P, Diana G, Vitiello F, Thiel G. Corticotropin-releasing factor triggers neurite outgrowth of a catecholaminergic immortalized neuron via cAMP and MAP kinase signalling pathways. *Eur J Neurosci.*, **13**, 1339–1348 (2001).

[7] Huang EJ, Reichardt LF. Neurotrophins: roles in neuronal development and function. *Annu Rev Neurosci.*, **24**, 677–736 (2001).

[8] Huber AB, Kolodkin AL, Ginty DD, Cloutier JF. Signaling at the growth cone: ligand-receptor complexes and the control of axon growth and guidance. *Annu Rev Neurosci.*, **26**, 509–563 (2003).

[9] Clagett-Dame M, McNeill EM, Muley PD. Role of all-trans retinoic acid in neurite outgrowth and axonal elongation. *J. Neurobiol.*, **66**, 739–56 (2006).

[10] Endo Y, Rubin JS. Wnt signaling and neurite outgrowth: Insights and questions. *Cancer Sci.*, **98**, 1311–1317 (2007).

[11] Lestanova Z, Bacova Z, Bakos J. Mechanisms involved in the regulation of neuropeptide-mediated neurite outgrowth: a minireview. *Endocr Regul.*, **50**, 72–82 (2016).

[12] Bennison SA, Blazejewski SM, Smith TH, Toyo-Oka K. Protein kinases: master regulators of neuritogenesis and therapeutic targets for axon regeneration. *Cell. Mol. Life Sci.*, **77**, 1511–1530 (2020).

[13] Antonell A, Lladó A, Altirriba J, Botta-Orfila T, Balasa M, Fernández M, Ferrer I, Sánchez-Valle R, Molinuevo JL. A preliminary study of the whole-genome expression profile of sporadic and monogenic early-onset Alzheimer's disease. *Neurobiol Aging.*, **34**, 1772–1778 (2013).

[14] Bossers K, Meerhoff G, Balesar R, van Dongen JW, Kruse CG, Swaab DF, Verhaagen J. Analysis of gene expression in Parkinson's disease: possible involvement of neurotrophic support and axon guidance in dopaminergic cell death. *Brain Pathol*., **19**, 91–107 (2009).

[15] Gilman SR, Chang J, Xu B, Bawa TS, Gogos JA, Karayiorgou M, Vitkup D. Diverse types of genetic variation converge on functional gene networks involved in schizophrenia. *Nat Neurosci.*, **15**, 1723–1728 (2012).

[16] Pinto D, Delaby E, Merico D, Barbosa M, Merikangas A, Klei L, Thiruvahindrapuram B, Xu X, Ziman R, Wang Z, et al. Convergence of genes and cellular pathways dysregulated in autism spectrum disorders. *Am J Hum Genet.*, **94**, 677–694 (2014).

[17] Svennerholm L. Distribution and fatty acid composition of phosphoglycerides in normal human brain. *J Lipid Res.*, **9**, 570–579 (1968).

[18] Tracey TJ, Steyn FJ, Wolvetang EJ, Ngo ST. Neuronal lipid metabolism: Multiple pathways driving functional outcomes in health and disease. *Front Mol Neurosci*., **23**, 11:10 (2018).

[19] Xicoy H, Wieringa B, Martens GJM. The role of lipids in Parkinson's disease. *Cells.*, **8**, 27 (2019).

[20] Van Meer G, Voelker DR, Feigenson GW. Membrane lipids: where they are and how they behave. *Nat Rev Mol Cell Biol.*, **9**, 112–124 (2008).

[21] Kim HY, Huang BX, Spector AA. Phosphatidylserine in the brain: metabolism and function. *Prog Lipid Res.*, **56**, 1–18 (2014).

[22] Makide K, Kitamura H, Sato Y, Okutani M, Aoki J. Emerging lysophospholipid mediators, lysophosphatidylserine, lysophosphatidylthreonine, lysophosphatidylethanolamine and lysophosphatidylglycerol. *Prostaglandins Other Lipid Mediat.*, **89**, 135–139 (2009).

[23] Choi JW, Chun J. Lysophospholipids and their receptors in the central nervous system. *Biochim Biophys Acta.*, **1831**, 20–32 (2013).

[24] Choi JW, Herr DR, Noguchi K, Yung YC, Lee CW, Mutoh T, Lin ME, Teo ST, Park KE, Mosley AN, Chun J. LPA receptors: subtypes and biological actions. *Annu Rev Pharmacol Toxicol.*, **50**, 157–186 (2010).

[25] Postma, F. R., Jalink, K., Hengeveld, T., and Moolenaar, W. H. Sphingosine-1-phosphate rapidly induces Rho-dependent neurite retraction: action through a specific cell surface receptor. *EMBO J.*, **15**, 2388–2392 (1996).

[26] Quarta S, Camprubí-Robles M, Schweigreiter R, Matusica D, Haberberger RV, Proia RL, Bandtlow CE, Ferrer-Montiel A, Kress M. Sphingosine-1-phosphate and the $S1P_3$ receptor initiate neuronal retraction via RhoA/ROCK associated with CRMP2 phosphorylation. *Front Mol Neurosci.*, **10**, 317 (2017).

[27] Sabogal-Guáqueta AM, Villamil-Ortiz JG, Arias-Londoño JD, Cardona-Gómez GP. Inverse phosphatidylcholine/phosphatidylinositol levels as peripheral biomarkers and phosphatidylcholine/lysophosphatidylethanolamine-phosphatidylserine as hippocampal indicator of postischemic cognitive impairment in Rats. *Front Neurosci.*, **12**, 989 (2018).

[28] Liu X, Li J, Zheng P, Zhao X, Zhou C, Hu C, Hou X, Wang H, Xie P, Xu G. Plasma lipidomics reveals potential lipid markers of major depressive disorder. *Anal Bioanal Chem.*, **408**, 6497–6507 (2016).

[29] Guo S, Zhou D, Zhang M, Li T, Liu Y, Xu Y, Chen T, Li Z. Monitoring changes of docosahexaenoic acid-containing lipids during the recovery process of traumatic brain injury in rat using mass spectrometry imaging. *Sci Rep.*, **7**, 5054 (2017).

[30] Kosicek M, Hecimovic S. Phospholipids and Alzheimer's disease: alterations, mechanisms and potential biomarkers. *Int J Mol Sci.*, **14**, 1310–1322 (2013).

[31] Van Blitterswijk WJ, De Veer G, Krol JH, Emmelot P. Comparative lipid analysis of purified plasma membranes and shed extracellular membrane vesicles from normal murine thymocytes and leukemic GRSL cells. *Biochim Biophys Acta.*, **688**, 495–504 (1982).

[32] Misra UK. Isolation of lysophosphatidylethanolamine from human serum. *Biochim Biophys Acta.*, **106**, 371–378 (1965).

[33] Nishina A, Kimura H, Sekiguchi A, Fukumoto RH, Nakajima S, Furukawa S. Lysophosphatidylethanolamine in *Grifola frondosa* as a neurotrophic activator via activation of MAPK. *J Lipid Res.*, **47**, 1434–1443 (2006).

[34] Park KS, Lee HY, Lee SY, Kim MK, Kim SD, Kim JM, Yun J, Im DS, Bae YS. Lysophosphatidylethanolamine stimulates chemotactic migration and cellular invasion in SK-OV3 human ovarian cancer cells: involvement of pertussis toxin-sensitive G-protein coupled receptor. *FEBS Lett.*, **581**, 4411–4416 (2007).

[35] Park SJ, Lee KP, Im DS. Action and signaling of lysophosphatidylethanolamine in MDA-MB-231 Breast Cancer Cells. *Biomol Ther (Seoul).*, **22**, 129–135 (2014).

[36] Montaner A, da Silva Santana TT, Schroeder T, Einicker-Lamas M, Girardini J, Costa MR, Banchio C. Specific phospholipids regulate the acquisition of neuronal and astroglial identities in post-mitotic cells. *Sci. Rep.*, **8**, 460 (2018).

[37] Villamil-Ortiz JG, Barrera-Ocampo A, Piedrahita D, Velásquez-Rodríguez CM, Arias-Londoño JD, Cardona-Gómez GP. BACE1 RNAi restores the composition of phosphatidylethanolamine-derivates related to memory improvement in aged 3xTg-AD mice. *Front Cell Neurosci.*, **10**, 260 (2016).

[38] Wuhanqimuge, Itakura A, Matsuki Y, Tanaka M, Arioka M. Lysophosphatidylcholine enhances NGF-induced MAPK and Akt signals through the extracellular domain of TrkA in PC12 cells. *FEBS Open Bio.*, **3**, 243–251 (2013).

[39] Bassa BV, Roh DD, Vaziri ND, Kirschenbaum MA, Kamanna VS. Lysophosphatidylcholine activates mesangial cell PKC and MAP kinase by PLCgamma-1 and tyrosine kinase-Ras pathways. *Am J Physiol.*, **277**, F328–337 (1999).

[40] Bennison SA, Blazejewski SM, Smith TH, Toyo-Oka K. Protein kinases: master regulators of neuritogenesis and therapeutic targets for axon regeneration. *Cell. Mol. Life Sci.*, **77**, 1511–1530 (2020).

[41] Park SJ, Lee KP, Kang S, Chung HY, Bae YS, Okajima F, Im DS. Lysophosphatidylethanolamine utilizes LPA_1 and CD97 in MDA-MB-231 breast cancer cells. *Cell. Signal.*, **25**, 2147–2154 (2013).

[42] Lee JM, Park SJ, Im DS. Lysophosphatidylethanolamine increases intracellular Ca^{2+} through LPA_1 in PC-12 neuronal cells. *Biochem Biophys Res Commun.*, **461**, 378–382 (2015).

[43] Lee JM, Park SJ, Im DS. Calcium signaling of lysophosphatidylethanolamine through LPA_1 in human SH-SY5Y neuroblastoma cells. *Biomol. Ther (Seoul).*, **25**, 194–201 (2017).

[44] Gschwendt M, Dieterich S, Rennecke J, Kittstein W, Mueller H, Johannes F. Inhibition of protein kinase C μ by various inhibitors. Differentiation from protein kinase c isoenzymes. *FEBS Lett.*, **392,** 77–80 (1996).

[45] Steinberg SF. Structural basis of protein kinase C isoform function. *Physiol. Rev.*, **88**, 1341–1378 (2008).

[46] Evenou JP, Wagner J, Zenke G, Brinkmann V, Wagner K, Kovarik J, et al. The potent protein kinase C-selective inhibitor AEB071 (sotrastaurin) represents a new class of immunosuppressive agents affecting early T-cell activation. *J Pharmacol Exp Ther.*, **330**, 792–801 (2009).

[48] Xu JY, Chen C. Endocannabinoids in synaptic plasticity and neuroprotection. *Neuroscientist.*, **21**, 152–168 (2015).

[49] B. Hille. G protein-coupled mechanisms and nervous signaling. *Neuron.*, **9**, 187–195 (1992).

[50] Oddo S, Caccamo A, Shepherd JD, Murphy MP, Golde TE, Kayed R, Metherate R, Mattson MP, Akbari Y, LaFerla FM. Triple-transgenic model of Alzheimer's disease with plaques and tangles: intracellular Aβ and synaptic dysfunction. *Neuron*, **39**, 409–421 (2003).

[51] Uemura T, Shiroshima T, Maeda A, Yasumura M, Shimada T, Fukata Y, Fukata M, Yoshida T. In situ screening for postsynaptic cell adhesion molecules during synapse formation. *J Biochem.*, **162**, 295–302 (2017).

[52] Schneider CA, Rasband WS, Eliceiri KW. NIH Image to ImageJ: 25 years of image analysis. *Nat Methods.*, **9**, 671–675 (2012).

[53] Cowan AK. Phospholipids as plant growth regulators. *Plant Growth Regul.*, **48**, 97–109 (2006).

[54] Meylaers K, Clynen E, Daloze D, DeLoof A, Schoofs L. Identification of 1-lysophosphatidylethanolamine (C(16:1)) as an antimicrobial compound in the housefly, Musca domestica. *Insect Biochem Mol. Biol.*, **34**, 43–49 (2004).

[55] Hong JH, Chung G and Cowan AK. Delayed leaf senescence by exogenous lyso-phosphatidylethanolamine: Towards a mechanism of action. *Plant Physiol. Biochem.*, **47**, 526–534 (2009).

[56] Liu X, Zheng P, Zhao X, Zhang Y, Hu C, Li J, Zhao J, Zhou J, Xie P, Xu G. Discovery and validation of plasma biomarkers for major depressive disorder classification based on liquid chromatography-mass spectrometry. *J Proteome Res* **,14**, 2322–2330 (2015).

[57] Sato, Y., Nakamura, T., Aoshima, K., and Oda, Y. Quantitative and wide-ranging profiling of phospholipids in human plasma by two-dimensional liquid chromatography/mass spectrometry. *Anal. Chem.*, **82**, 9858–9864 (2010).

[58] Yamamoto, Y., Sakurai, T., Chen, Z., Furukawa, T., Gowda, S.G.B., Wu, Y., Nouso, K., Fujii, Y., Yoshikawa, Y., Chiba, H., and Hui, S.P. Analysis of serum lysophosphatidylethanolamine levels in patients with non-alcoholic fatty liver disease by liquid chromatography-tandem mass spectrometry.

Anal. Bioanal. Chem. **413**, 245–254 (2021).

[59] Péter, M., Török, W., Petrovics-Balog, A., Vígh, L., Vécsei, L., and Balogh, G. Cerebrospinal fluid lipidomic biomarker signatures of demyelination for multiple sclerosis and Guillain-Barré syndrome. *Sci*. *Rep*. **10**, 18380 (2020).

[60] Trim PJ, Atkinson SJ, Princivalle AP, Marshall PS, West A, Clench MR. Clench Matrix-assisted laser desorption/ionisation mass spectrometry imaging of lipids in rat brain tissue with integrated unsupervised and supervised multivariant statistical analysis. *Rapid Commun Mass Spectrom.*, **22**, 1503–1509 (2008).

[61] Bryan, L., Kordula, T., Spiegel, S., and Milstien, S. Regulation and functions of sphingosine kinases in the brain. *Biochim Biophys Acta*., **1781**, 459–466 (2008).

[62] Wackerlig J, Köfeler HC, Korz V, Hussein AM, Feyissa DD, Höger H, Urban E, Langer T, Lubec G, Lubec J. Differences in hypothalamic lipid profiles of young and aged male rats with impaired and unimpaired spatial cognitive abilities and memory. *Front Aging Neurosci.*, **12**, 204 (2020).

[63] Naor Z and Huhtaniemi I. Interactions of the GnRH receptor with heterotrimeric G proteins. *Front Neuroendocrinol* **34**, 88–94 (2013).

[64] Sabogal-Guáqueta AM, Posada-Duque R, Cortes NC, Arias-Londoño JD, Cardona-Gómez GP. Changes in the hippocampal and peripheral phospholipid profiles are associated with neurodegeneration hallmarks in a long-term global cerebral ischemia model: Attenuation by Linalool. *Neuropharmacology*, **135**, 555–571 (2018).

[65] Llansola M, Monfort P, FelipoV. Inhibitors of phospholipase C prevent glutamate neurotoxicity in primary cultures of cerebellar neurons. *J Pharmacol Exp Ther*., **292**, 870–876 (2000).

[66] Tang Z, Li S, Han P, Yin J, Gan Y, Liu Q, Wang J, Wang C, Li Y, Shi J. Pertussis toxin reduces calcium influx to protect ischemic stroke in a middle cerebral artery occlusion model. *J Neurochem.*, **135**, 998–1006 (2015).

[67] Stanciu M, Wang Y, Kentor R, Burke N, Watkins S, Kress G, Reynolds I, Klann E, Angiolieri MR, Johnson JW, DeFranco DB. Persistent activation of ERK contributes to glutamate-induced oxidative toxicity in a neuronal cell line and primary cortical neuron cultures. *J Biol Chem.*, **275**, 12200–12006 (2000).

[68] Q. Huang, H. Lei, M. Dong, Y. Wang. Quantitative analysis of 10 classes of phospholipids by ultrahigh-performance liquid chromatography tandem triple-quadrupole mass spectrometry. *Analyst*, **144**, 3980–3987 (2019).

[69] Aoki, J. Mechanisms of lysophosphatidic acid production. *Semin*. *Cell Dev*. *Biol*. **15**, 477–489 (2004).

[70] Shindou, H., and Shimizu, T. Acyl-CoA: lysophospholipid acyltransferases. *J. Biol*. *Chem*. **284**, 1–5(2009).

[71] Subramaniam, S., and Unsicker, K. ERK and cell death: ERK1/2 in neuronal death. *FEBS J*. **277**, 22–29 (2010).

[72] Yue, J., and López, J.M. Understanding MAPK signaling pathways in apoptosis. *Int*. *J*. *Mol*. *Sci*. **21**, 2346 (2020).

[73] P. Maher. How protein kinase C activation protects nerve cells from oxidative Stress-induced cell death. *J. Neurosci.*, **21**, 2929–2938 (2001).

[74] J. Lewerenz, P. Maher. Chronic glutamate toxicity in neurodegenerative diseases—What is the evidence? *Front. Neurosci*., **9**, 469 (2015).

[75] Shindou H., Koso H., Sasaki J., Nakanishi H., Sagara H., Nakagawa KM., Takahashi Y., Hishikawa D., Iizuka-Hishikawa Y., Tokumasu F., Noguchi H., Watanabe S., Sasaki T., Shimizu T. Docosahexaenoic acid preserves visual function by maintaining correct disc morphology in retinal photoreceptor cells. *J Biol Chem.*, **292**, 12054–12064 (2017).

[76] Yamamoto T., Endo J., Kataoka M., Matsuhashi T., Katsumata Y., Shirakawa K., Yoshida N., Isobe S., Moriyama H., Goto S., Yamashita K., Nakanishi H., Shimanaka Y., Kono N., Shinmura K., Arai H., Fukuda K., Sano M. Decrease in membrane phospholipids unsaturation correlates with myocardial diastolic dysfunction. *PLoS One.*, **13**, e0208396 (2018).

[77] Bligh, E.G. & Dyer, W.J. A rapid method of total lipid extraction and purification. *Canadian journal of biochemistry and physiology*, **37**, 911–917 (1959).

List of publications

1. **Kazutoshi Hisano**, Shiori Kawase, Tetsuhiko Mimura, Hironori Yoshida, Hiroki Yamada, Hisao Haniu, Tamotsu Tsukahara, Taiga Kurihara, Yoshikazu Matsuda, Naoto Saito, Takeshi Uemura. Structurally different lysophosphatidylethanolamine species stimulate neurite outgrowth in cultured cortical neurons via distinct G-protein-coupled receptors and signaling cascades. *Biochemical and Biophysical Research Communications*, **534**, 179–185 (2021). DOI: 10.1016/j.bbrc.2020.11.119.

2. **Kazutoshi Hisano**, Hironori Yoshida, Shiori Kawase, Tetsuhiko Mimura, Hisao Haniu, Tamotsu Tsukahara, Taiga Kurihara, Yoshikazu Matsuda, Naoto Saito, Takeshi Uemura. Abundant oleoyl-lysophosphatidylethanolamine in brain stimulates neurite outgrowth and protects against glutamate toxicity in cultured cortical neurons [published online ahead of print April 5, 2021]. *The Journal of Biochemistry.* DOI: 10.1093/jb/mvab046.

6 Acknowledgments

I am deeply grateful to Associate Prof. Takeshi Uemura and Prof. Naoto Saito for the opportunity of being a member of their research group at Shinshu University in Nagano; for their support, guidance and suggestions of improvement during the experimental and writing phases of this research.

I am deeply grateful to my supervisor, Assistant Prof. Akari Takeuchi for providing guidance.

I greatly thank to Associate Prof. Hisao Haniu for useful discussion about phospholipid.

I would like to express my sincere thanks to Mrs. Shiori Kawase, your kind support in spinning experiments really helped me a lot.

I would like to thank the “Biocompatible System Engineering” members. The daily discussions with all of you had a lot of positive effects on me.

Finally, I would like to express sincere thanks to “STELLA CHEMIFA CORPORATION” for giving me such a wonderful opportunity.